Joint RIS-Aided Precoding and Multislot Scheduling for Maximum User Admission in Smart Cities

Progress Zivuku, *Graduate Student Member, IEEE*, Steven Kisseleff, *Senior Member, IEEE*, Van-Dinh Nguyen, *Senior Member, IEEE*, Wallace A. Martins, *Senior Member, IEEE*, Konstantinos Ntontin, *Member, IEEE*, Symeon Chatzinotas, *Fellow, IEEE*, and Björn Ottersten, *Fellow, IEEE*

***Abstract*— Reconfigurable intelligent surfaces (RISs) have emerged as a game-changing technology to improve wireless network performance by intelligently manipulating and customizing the physical propagation environment. Such capability is especially important for the application of smart cities as it increases wireless service offers and quality to end-users. In this paper, we aim to maximize the number of served users in a challenging RIS-aided smart city street by jointly optimizing the multislot scheduling, precoding, and passive RIS-based beamforming design under quality of service and power constraints. Multislot scheduling is introduced in order to benefit from additional time diversity and thus better exploit the available degrees of freedom. The formulated problem is a mixed integer nonlinear programming, which is NP-hard. To solve the problem with affordable complexity, we develop an efficient iterative algorithm based on binary variable relaxation, alternating optimization, and successive convex approximation techniques. Simulation results demonstrate the superiority of the proposed design over the design without RIS and the design without scheduling, especially in the presence of a large number of users. In addition, results illustrate that by introducing a quality of service margin, the proposed design can improve its robustness to outdated channel state information in mobility scenarios.**

***Index Terms*— Reconfigurable intelligent surfaces, smart cities, quality of service, precoding, scheduling, successive convex approximation.**

I. Introduction

A. Motivation

THE growing demand for a fully connected and intelligent world has driven research to advance communication technologies beyond 5G wireless networks [1]. Future wireless networks are expected to satisfy certain quality of service (QoS) requirements, such as improved user data rate, massive device connectivity, and high energy efficiency. This is to ensure that sufficient performance and quality levels can be provided for various end-applications [2]. Recently, reconfigurable intelligent surfaces (RISs) have emerged as a promising technology to meet the stringent demands of beyond 5G wireless networks and to advance the vision of smart radio environments [3]. Specifically, RIS is a software-controllable meta-surface that consists of a number of passive reconfigurable reflecting elements. The RIS elements are capable of passively reflecting electromagnetic signals to users without the need for energy-demanding radio frequency chains and amplifiers [4]. The amplitude/phase-shift of individual reflective elements of RIS can be adjusted to change the strength/direction of the reflected signals for a variety of applications including beamforming, interference nulling, security engineering, and spatial multiplexing [5], [6], [7], [8]. The controllable signal reflections from RISs are highly beneficial for ensuring seamless connectivity, especially in complex propagation environments, *e.g.* dense urban environments where signal propagation may often be blocked by high-rise buildings and a large number of city infrastructures [9]. These controllable signal reflections make the deployment of RIS quite promising in the concept of smart cities.

The emerging concept of smart cities seeks to integrate information communication technology (ICT) and other related technologies in the urban environment to improve the efficiency of city operations and QoS for the citizens [10]. Smart cities are a response to the challenge of urbanization which is leading to rising demands in communications, thereby posing challenges for cities to provide sufficient connectivity for their businesses and citizens [11]. Further, applications in the smart city involve an exchange of crucial and sensitive information under system constraints [12]. There are critical services (*e.g.* government, medical, and businesses) that may require immediate service availability. In this case, it is the telecommunications (telecom) operator's responsibility to ensure the provision of sufficient connectivity to as many users as possible under acceptable QoS conditions. Accordingly, user admission maximization is a promising design criterion. Typically, this can be achieved via the deployment of a large number of active network components e.g. active base station (BS) and access points, which leads to network densification, increased energy consumption, and additional

Manuscript received 21 March 2023; revised 27 July 2023; accepted 23 September 2023. Date of publication 4 October 2023; date of current version 17 January 2024. This work is funded by the Luxembourg National Research Fund (FNR) as part of the CORE program under project RISOTTI C20/IS/14773976. The work of Van-Dinh Nguyen was supported in part by the VinUniversity Seed Grant Program. An earlier version of this paper was presented in part at the IEEE Wireless Communications and Networking Conference (WCNC) 2022 [1]. The associate editor coordinating the review of this article and approving it for publication was M. Bhatnagar. *(Corresponding author: Progress Zivuku.)*

Progress Zivuku, Steven Kisseleff, Konstantinos Ntontin, Symeon Chatzinotas, and Björn Ottersten are with the Interdisciplinary Centre for Security, Reliability and Trust (SnT), University of Luxembourg, 4365 Esch-sur-Alzette, Luxembourg (e-mail: progress.zivuku@uni.lu; steven.kisseleff@uni.lu; kostantinos.ntontin@uni.lu; symeon.chatzinotas@uni.lu; bjorn.ottersten@uni.lu).

Van-Dinh Nguyen is with the College of Engineering and Computer Science and the Center for Environmental Intelligence, VinUniversity, Hanoi 100000, Vietnam (e-mail: dinh.nv2@vinuni.edu.vn).

Wallace A. Martins is with ISAE-SUPAERO, Université de Toulouse, 31058 Toulouse, France (e-mail: wallace.martins@isae-supaero.fr).

Color versions of one or more figures in this article are available at https://doi.org/10.1109/TCOMM.2023.3321731.

Digital Object Identifier 10.1109/TCOMM.2023.3321731

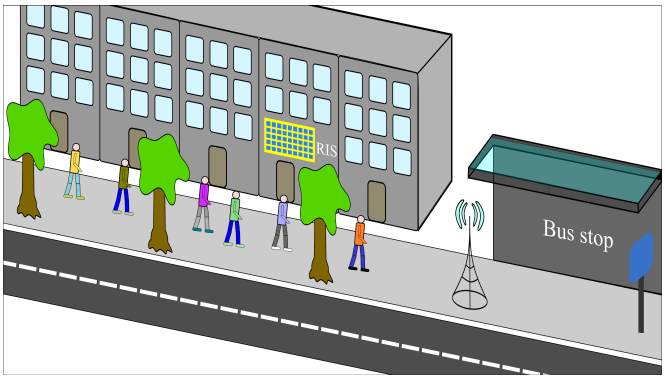

Fig. 1. Smart city street scenario.

hardware complexity. In this context, deploying RIS may lower the required communication infrastructure by offering increased energy efficiency, coverage, spectral efficiency, channel rank improvement, and minimized exposure to electromagnetic radiation in outdoor areas. RISs can be easily placed on surfaces in the city environment, such as buildings, billboards, public transport vehicles, and unmanned aerial vehicles. This can result in better public service accessibility, digital advancement of the urban environment, and monitoring of several societal processes and city assets [12], [13]. Upon deployment of RIS, the smart city communication environment will become partially controllable/smart, which as a result enables a symbiotic relationship between the smart city and its communication infrastructures [12].

Intensive studies in RIS-aided wireless communications were carried out for many system settings, including single-user/multiuser/multicell systems, physical layer security, millimeter wave (mmWave) communications, and so on, due to the aforementioned advantages [14], [15], [16], [17], [18], [19], [20], [21]. Most published works on RIS studied the joint optimization of active and passive beamforming under various design objectives. Most of these works studied the minimization of total transmit power [22], [23], [24], [25], signal to interference plus noise ratio (SINR) maximization [26] and network sum-rate maximization [27], [28], [29]. However, none of these works addressed user admission maximization which is fundamental in smart cities. The authors in [30] studied the ability of RIS to improve the channel matrix rank, resulting in a notable increase in capacity gains even in line-of-sight (LoS) propagation. This confirms that RIS-aided network is effective in significantly increasing the number of users a network can support. On the other hand, the scheduling of users in RIS-aided networks has been rarely addressed so far. Conventional networks (without RIS) carried out a thorough investigation on resource allocation mainly focusing on scheduling, admission control, user selection and precoding over the past few decades [31], [32], [33], [34], [35], [36]. The formulated problems are usually combinatorial in nature and thus difficult to solve. These problems become even more challenging if we consider a RIS-aided network. The authors in [37], [38], and [39] studied scheduling in RIS-aided networks using machine learning-based techniques. The focus of these works was to maximize the weighted sum-rate and maximizing the minimum bit-rate.

In this work, we focus on maximizing the admission of users, *i.e.*, the number of users served in a smart city street via joint multislot scheduling, precoding, and passive RIS-based beamforming. Multislot scheduling refers to time-domain multiplexing. Although the traditional scheduling of users is often orthogonal, *i.e.*, one user per time slot, in this work we consider a generalized approach, where multiple users receive different data packets in the same time slot. In order to avoid co-channel interference in this case, we employ multiuser precoding, which is a method to exploit available spatial diversity. Since the spatial diversity of the system may not always be sufficient, we introduce a RIS, which can have a better spatial resolution of the channels. The RIS performs passive beamforming to enhance the spatial diversity and thus improve the performance of the multiuser precoding. Passive beamforming refers to the adaptation of the RIS reflection pattern by manipulating the impedance of the RIS's reflecting elements without the need for active electronic components, *i.e.*, power amplifiers. The proposed scheme provides the flexibility to efficiently schedule users across multiple time slots for improved performance. This is highly beneficial in networks where the number of users demanding access to the network is larger than the number of available base station (BS) antennas. In this case, there is less diversity to schedule users in one-time slot. Simulation results in our previous work [1], demonstrated that it may not always be possible to serve all users with desired QoS in one-time slot via joint precoding and passive beamforming design, especially if the number of users approaches the number of BS antennas. Accordingly, it is highly challenging for conventional multi-user precoding design to serve all users with a sufficiently high QoS. Further, in practical scenarios the users may request a certain number of data packets per time frame, i.e. they may not need to be served continuously. This motivates the introduction of multislot scheduling, which can help to exploit time diversity in addition to the enhanced spatial diversity enabled by RIS. While this problem is very important in the context of smart cities, to the best of our knowledge, it has not yet been addressed in the literature. Further, the formulated problem of maximizing the number of served users is quite challenging as compared to the existing literature as it involves the joint optimization of multislot scheduling, precoding and RIS-based beamforming.

B. Contributions

Considering the demands on the urban area (e.g. smart cities) outlined above, our main goal is to study a practical scenario of a smart city with a realistic distribution of users and a relevant performance objective. Specifically, we focus on maximizing the number of served users in a challenging RIS-aided smart city street subject to QoSs and power constraints. We maximize the number of users by jointly optimizing the multislot scheduling, precoding and passive beamforming design. The joint multislot scheduling of users may help to utilize both spatial and time diversities, such that more users can be potentially accommodated. As illustrated in

Fig. 1, we consider a scenario where users walk on a smart city street toward a common target (e.g. metro stations or bus stops), where the base station (BS) is deployed. Here, the realistic objective for a smart city application is to provide quality service to as many users as possible on a resource-constrained network. The location of the users can be random on the straight line in front of the BS. In this case, providing quality service to a large number of users is particularly challenging since the distribution of users on the city street and the propagation environment do not provide a sufficient angular spread for the BS to serve all users with an acceptable signal quality due to co-channel interference, see Fig 1. Accordingly, we propose the deployment of a RIS on a building facade of the same street in order to provide an opportunity for improving spatial diversity. Moreover, a distinct benefit of RIS deployment in this scenario may arise from the fact that the RIS may have a better view of the users as compared to BS. To the best of our knowledge, this scenario has not been considered in the literature. Further, it is important to note that RISs can be implemented in different ways including the simultaneously transmitting and reflecting (STAR)-RIS which is capable of supporting the 360° coverage [40]. However, in the considered scenario, the deployment of RIS at the building facade dictates the location of BS and users in the half-space of RIS, such that the transmitting functionality of STAR-RIS is not needed. Accordingly, we focus on purely reflective RIS in the following.

In summary, the main contributions of this paper are as follows:

- For a practical scenario of a smart city street with limited spatial diversity, we propose to maximize the admission of users, i.e. the number of served users under QoS and power constraints. Accordingly, we formulate a novel optimization problem to maximize the number of users served in a network via a joint optimization of multislot scheduling, precoding and passive RIS-based beamforming. The novelty of this optimization problem lies in the utilization of spatial and time diversities in the presence of RIS as well as the objective of maximizing the number of users that can be accommodated by the system. In addition, this design strategy is tailored for the target application in contrast to conventional multi-user designs based on sum-rate maximization or power consumption minimization. The conventional multi-user designs based on sum-rate maximization are network-centric designs with a focus on accommodating higher volumes of data traffic in the network. In contrast to the network-centric design, the proposed design strategy prioritizes the provision of connectivity to a large number of users (*i.e.,* it maximizes the number of users that the network can support at their desired SINR). This user-centric design is appealing from a network operator's perspective since it is more service-oriented [40]. Specifically, this design strategy utilizes spatial and time diversities in the presence of RIS to maximize the admission of users in a smart city. User admission maximization results in a more fair distribution of resources, enhancing user satisfaction. In scenarios where there is a large number of users demanding access to a resource-constrained network, especially in smart cities, this design strategy ensures that an increased user base can access the network and benefit from its services. Specifically, it helps to increase the network service availability and coverage which is very important for the critical services in smart cities. In addition, this user-centric design is crucial for network deployments that intend to facilitate emergency communication or offer ubiquitous connectivity.
- The resulting optimization problem is a mixed-integer nonlinear program (MINLP), which is non-convex and thus difficult to solve in polynomial time using the methods of combinatorial programming and convex optimization. In order to solve this problem, we develop a simple yet efficient iterative algorithm. Firstly, we relax the binary variables and then penalize the objective using two penalty functions to ensure binary solutions at convergence. Next, we resort to alternating optimization (AO) to tackle the coupling between optimization variables. Specifically, we decompose the problem into two tractable sub-problems. Finally, we tackle the non-convexity of the sub-problems by combining the tools from mathematical transformations and successive convex approximation (SCA) [41]. Simulation results demonstrate the effectiveness of the proposed design in terms of the average number of served users under various conditions as compared to the design without RIS and without scheduling.
- We investigate the impact of outdated channel state information (CSI) on the overall system performance. In this context, we introduce a QoS margin to improve the robustness of the proposed design against the outdated CSI. In particular, for a given correlation coefficient that depends on the user mobility (i.e. a large correlation coefficient pertains to low mobility and a low correlation coefficient pertains to high mobility), simulation results show that a QoS margin results in better performance and improves the robustness of the system against outdated CSI.

We introduce the considered RIS-aided system model in Section II and carry out an optimization problem formulation for a multislotted RIS-aided wireless system in Section III. In Section IV, we present an alternating optimization algorithm based on SCA to solve the formulated problem. In this section, we also detail the derivation of the proposed solution. Numerical results are presented in Section V to evaluate the effectiveness of the proposed design against benchmark schemes. Finally, conclusions are drawn in Section VI.

Notations: Scalars are denoted by italic letters, vectors and matrices are denoted by bold-face lower-case and upper-case letters, respectively. $\mathbb{C}^{x\times y}$ denotes the space of $x\times y$ complex-valued matrices. $|\cdot|, ||\cdot||, (\cdot)^H, (\cdot)^T, \mathrm{Re}\{\cdot\}$ and $\arg(\cdot)$ denote absolute value, Euclidean norm, Hermitian transpose, transpose, real part and the phase, respectively. diag(.) produces a square matrix with the elements of its argument on the main diagonal and zeros otherwise. $\mathscr{K}$ denotes a set of K elements.

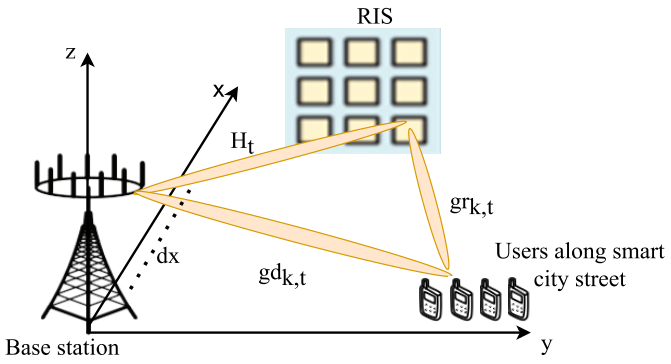

Fig. 2. RIS-aided multiuser MISO system in a smart city scenario.

II. System Model

We consider a downlink transmission of a multislotted RIS-aided multiuser multiple-input single-output (MISO) system in a smart city street scenario. From a set $\mathcal{K} \triangleq \{1,\dots,K\}$ of K users, as many users as possible should be served by the BS with the help of a RIS deployed on a building facade. Each user is equipped with a single-antenna user equipment (UE). The BS is equipped with M transmit antennas and the RIS is equipped with a set $\mathcal{N} \triangleq \{1,\dots,N\}$ of N reflective elements. We consider a scheduling strategy for a system where a large number of users ($K > M$) simultaneously request access to the network. In this case, it is very likely that the transmitter cannot serve all users at once, only a subset $\mathcal{K}_t$ of users in each time slot can be scheduled for transmission. Accordingly, users are served in a time window comprised of a set $\mathcal{T} \triangleq \{1,\dots,T\}$ of T time slots. To be able to perform the joint multislot scheduling, precoding and passive beamforming, CSI is required for the observed time window. Let $\mathbf{H}_t \in \mathbb{C}^{N\times M}$, $\mathbf{g}_{\mathrm{r}_{k,t}} \in \mathbb{C}^{1\times N}$ and $\mathbf{g}_{\mathrm{d}_{k,t}} \in \mathbb{C}^{1\times M}$ denote the BS to RIS, RIS to k-th user and BS to k-th user in time slot t channels, respectively. Further, we consider a linear transmit beamforming at the BS, where the k-th user in time slot t is assigned a dedicated beamforming vector $\mathbf{w}_{k,t} \in \mathbb{C}^{M\times 1}$. The complex baseband signal at the BS can be expressed as $\mathbf{x}_t = \sum_{k\in\mathcal{K}} \mathbf{w}_{k,t} s_{k,t}, \forall t \in \mathcal{T}$, where $s_{k,t}$ denotes the data symbol intended to user k in time slot t, which is assumed to have zero mean and unit variance. In this case, $s_{k,t}$ is assumed independent and identically distributed (i.i.d) across k. Accordingly, the total transmit power at the BS in time slot t is:

$$P_{\mathrm{tot}}(t) = \sum_{k\in\mathcal{K}} ||\mathbf{w}_{k,t}||^2. \tag{1}$$

Let $\theta_{n,t} \in [0, 2\pi]$ be the phase shift induced by the nth reflective element of the RIS in time slot t. We denote by $\mathbf{\Theta}_t = \mathrm{diag}([e^{j\theta_{1,t}} \dots e^{j\theta_{n,t}} \dots e^{j\theta_{N,t}}])$ the RIS-based beamforming matrix that captures the reflective properties of RIS elements. For simplicity, the amplitude of the reflective coefficient is set to $1, \forall n$ [42], [43]. The signal received at the k-th user in time slot t can be expressed as

$$y_{k,t} = (\mathbf{g}_{\mathrm{r}_{k,t}} \mathbf{\Theta}_t \mathbf{H}_t + \mathbf{g}_{\mathrm{d}_{k,t}}) \sum_{i\in\mathcal{K}} \mathbf{w}_{i,t} s_{i,t} + v_{k,t}, \quad \forall k,t \tag{2}$$

where $v_{k,t}$ is the additive white Gaussian noise (AWGN) at the receiver with zero mean and variance σ_k^2, *i.e.* $v_{k,t} \sim \mathcal{CN}(0, \sigma_k^2)$. All signals from other users are treated as interference by the k-th user.

In this work, we consider a passive RIS, and therefore only the CSI of the effective channels (i.e. $\mathbf{h}_{k,t} = \mathbf{g}_{\mathrm{r}_{k,t}} \mathbf{\Theta}_t \mathbf{H}_t + \mathbf{g}_{\mathrm{d}_{k,t}}$) is acquired at BS to perform beamforming for downlink transmission. This can be done by uplink channel estimation, where all users transmit their orthogonal pilot sequences (e.g. Walsh-Hadamard sequences) to BS for performing channel estimation.[1] Moreover, we consider quasi-static block fading for all channels of the network.[2] In practice, the large-scale parameters are varied much more slowly than small-scale fading channels (i.e. they can be constant for about 40 coherence intervals of small-scale fading [44]). Accordingly, we assume that the channels have a coherence time corresponding to the window size, for which the channels can be viewed as nearly constant. This is a typical assumption for low-mobility scenarios, which is justified by the slow motion of the users on the street. In this case, the channels can be predicted accurately up to a few slots [45]. The assumption of block fading channel holds even for large sizes of RIS. For instance, the channel coherence time for a 2.4 Ghz carrier frequency with a user velocity of 1.4 m/s is $T_c = 89.2$ ms. This is much greater than the symbol duration in LTE which is 7.1 μs [46]. In this case, the channel estimation of a large-size RIS, one element at a time, can be accommodated [46]. Accordingly, the SINR for k-th user in time slot t is denoted by

$$\gamma_{k,t}(\mathbf{W},\boldsymbol{\theta}) = \frac{|(\mathbf{g}_{\mathrm{r}_{k,t}} \mathbf{\Theta}_t \mathbf{H}_t + \mathbf{g}_{\mathrm{d}_{k,t}})\mathbf{w}_{k,t}|^2}{\sum\limits_{i\in\mathcal{K}\setminus\{k\}} |(\mathbf{g}_{\mathrm{r}_{k,t}} \mathbf{\Theta}_t \mathbf{H}_t + \mathbf{g}_{\mathrm{d}_{k,t}})\mathbf{w}_{i,t}|^2 + \sigma_k^2}, \quad \forall k,t \tag{3}$$

where $\mathbf{W} \triangleq [\mathbf{w}_{k,t}]_{k\in\mathcal{K},t\in\mathcal{T}}$ is the three-dimensional tensor that contains all the precoding vectors for all users in all time slots. Accordingly, the dimensions of $\mathbf{W}$ correspond to the BS transmit antennas, users and time slots. Further, $\boldsymbol{\theta} \triangleq [\theta_{n,t}]_{n\in\mathcal{N},t\in\mathcal{T}}$ is a matrix that contains all the RIS phase shift (passive beamforming) vectors in all time slots. The spectral efficiency of the k-th user in slot t is

$$R_{k,t} = \log(1 + \gamma_{k,t}(\mathbf{W},\boldsymbol{\theta})), \quad \forall k,t. \tag{4}$$

III. Problem Formulation

The ultimate goal of this work is to maximize the admission of users, *i.e.*, the number of served users in a time window comprised of T time slots, subject to QoS and power constraints. Toward defining our optimization problem, we first introduce binary variables $\boldsymbol{\epsilon} \triangleq [\epsilon_{k,t}]_{k\in\mathcal{K},t\in\mathcal{T}}$ and $\boldsymbol{\phi} \triangleq [\phi_k]_{k\in\mathcal{K}}$.

[1]The details of uplink channel estimation are beyond the scope of this work.

[2]Our previous work has demonstrated that the diversity of the MIMO channel is sufficient to simultaneously serve a large number of users only in the presence of strong non-LOS channel components [1]. In this case, the spatial diversity is sufficient to accommodate a large number of users despite a very poor angular resolution.

Definition 1: Let us introduce $\boldsymbol{\epsilon}$ as a binary matrix (illustrated in Fig. 3) that contains the state of each user in each time slot, represented by its element $\epsilon_{k,t}$. The value of $\epsilon_{k,t}$ is equal to one if the condition $\gamma_{k,t}(\mathbf{W},\boldsymbol{\theta}) \geq \gamma_{\text{th}}$ is satisfied; and $\epsilon_{k,t} = 0$, otherwise. This is generally expressed as $\gamma_{k,t}(\mathbf{W},\boldsymbol{\theta}) \geq \epsilon_{k,t}\gamma_{\text{th}}$ with $\epsilon_{k,t} \in \{0,1\}$.

The activation of users is according to the scheduling that is optimized based on the expected received SINR. The optimization provides an output of the user assignment to the time slots, *i.e.* their activation pattern and the respective precoding vectors.

Definition 2: $\boldsymbol{\phi}$ is a vector that contains the state of each user in a time window, where ϕ_k is an element of vector $\boldsymbol{\phi}$. The value of ϕ_k is equal to one if user k is served in the whole time window, i.e. $\sum_{t=1}^{T} \epsilon_{k,t} \geq \alpha_{\text{th}}$, where α_{th} is the minimum number of time slots that the user should occupy to satisfy the given QoS constraints in terms of the average data rate; and $\phi_k = 0$, otherwise. This is generally expressed as $\sum_{t\in\mathscr{T}} \epsilon_{k,t} \geq \phi_k\alpha_{\text{th}}, \forall k \in \mathscr{K}$.

Unlike traditional orthogonal multiplexing methods, the achievable rate per user (or capacity per user) in this work does not reduce with the number of time slots or number of users, since each user is considered served only if data is received in a certain percentage of the total number of time slots. In other words, if the user needs to be served in 50% of time slots, then the rate of this user remains unchanged with 10 time slots or 100 time slots. Accordingly, the QoS of each user remains unchanged, even if the number of users or the number of time slots changes over time.

Following the above definitions, the joint multislot scheduling, precoding and passive RIS-based beamforming optimization problem for maximizing the number of served users in an observed time window can be mathematically formulated as[3]

$$\mathscr{P}: \quad \max_{\mathbf{W},\boldsymbol{\theta},\boldsymbol{\epsilon},\boldsymbol{\phi}} \quad \sum_{k\in\mathscr{K}} \phi_k \tag{5a}$$

$$\text{s. t.} \quad \gamma_{k,t}(\mathbf{W},\boldsymbol{\theta}) \geq \epsilon_{k,t}\gamma_{\text{th}}, \quad \forall k \in \mathscr{K},\ \forall t \in \mathscr{T} \tag{5b}$$

$$\sum_{k\in\mathscr{K}} \|\mathbf{w}_{k,t}\|^2 \leq P^{\max}, \quad \forall t \in \mathscr{T} \tag{5c}$$

$$0 \leq \theta_{n,t} \leq 2\pi, \quad \forall n \in \mathscr{N},\ \forall t \in \mathscr{T} \tag{5d}$$

$$\epsilon_{k,t} \in \{0,1\}, \quad \forall k \in \mathscr{K},\ \forall t \in \mathscr{T} \tag{5e}$$

$$\phi_k \in \{0,1\}, \quad \forall k \in \mathscr{K} \tag{5f}$$

$$\sum_{t\in\mathscr{T}} \epsilon_{k,t} \geq \phi_k\alpha_{\text{th}}, \quad \forall k \in \mathscr{K} \tag{5g}$$

where $P^{\max}$ is the total power available at the BS. The constraints are explained in detail as follows:

[3]The joint multislot scheduling, precoding and passive beamforming problem in (5) can be reduced to a joint precoding and passive beamforming problem if we set $T = 1$. In that case, constraints (5f) and (5g) will become redundant. The resulting problem is equivalent to the problem solved in [1]. However, we observe that despite a thorough optimization, it is not possible to serve all users in one-time slot, especially when there is a large number of users demanding access to the network. It is also important to note that the recently introduced rate splitting (RSMA) [47] has emerged as a promising multiple access scheme and can be exploited to improve the system performance in the considered scenario. However, the analysis of its advantages or disadvantages with respect to the number of users is beyond the scope of this work.

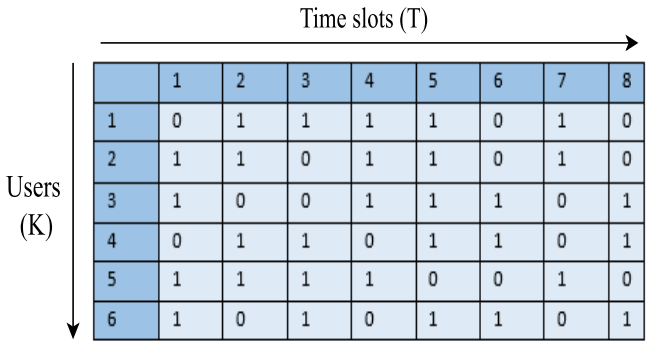

	1	2	3	4	5	6	7	8
1	0	1	1	1	1	0	1	0
2	1	1	0	1	1	0	1	0
3	1	0	0	1	1	1	0	1
4	0	1	1	0	1	1	0	1
5	1	1	1	1	0	0	1	0
6	1	0	1	0	1	1	0	1

Fig. 3. An illustration of how users are combined differently in different time slots.

- *SINR constraint per-slot (5b)*: Constraint (5b) provides per-slot QoS requirement. The term $\epsilon_{k,t}$ indicates that the SINR should satisfy this constraint only if the k-th user is served in time slot t; Otherwise, the threshold $\epsilon_{k,t}\gamma_{\text{th}}$ becomes zero and this constraint is disabled.
- *Power constraint (5c)* : Constraint (5c) ensures that the power allocated to users is less than or equal to the available power at the BS ($P^{\max}$) for all time
- *RIS phase shifts (5d)*: The phase shifts of RIS must be between 0 and 2π.
- *State of user in a slot (5e)*: Constraint (5e) describes whether or not user k is served in time slot t.
- *State of user in a time window (5f)*: Constraint (5f) describes the state of the k-th user in a time window.
- *Users' service requirement in a time window (5g)* : Constraint (5g) ensures that user k satisfies the QoS requirement in a time window only if it has been served at least in α_{th} time slots. If ϕ_k is zero, the minimum number of time slots $\phi_k\alpha_{\text{th}}$ becomes zeros and this constraint is disabled.

We can note that problem $\mathscr{P}$ is a mixed-integer non-convex problem due to the non-convexity of constraint (5b), while constraints (5e) and (5f) are binary in nature. Accordingly, the formulated joint multislot scheduling, precoding and passive beamforming problem described in (5) is an MINLP. In this case, it may not be possible to provide a globally optimal solution in polynomial time, and standard convex optimization techniques are not applicable. Accordingly, we resort to a low-complexity algorithm to solve the formulated challenging problem. One of the most commonly used approaches to solve problem (5) is to transform and relax integer variables to continuous ones so as to obtain a continuous optimization problem. However, even after such a relaxation, problem (5) remains non-convex. This is due to the coupling of precoding and passive beamforming variables in the SINR constraint (5b). To address these challenges, firstly, we relax binary variables to continuous ones (*i.e.* $\epsilon_{k,t} \in [0,1], \forall k, \forall t$ and $\phi_k \in [0,1], \forall k$), then we split the problem into two tractable subproblems and apply mathematical transformations and SCA to each of them.

IV. Proposed Alternating Optimization Algorithm

In this section, we present an efficient iterative algorithm to tackle the challenging problem in 5 effectively. Firstly,

we relax the binary variables in constraint (5e) and (5f). Secondly, we propose an alternating optimization by decomposing the problem into two tractable subproblems (precoding design and phase shift optimization). Lastly, to tackle the non-convexity of the subproblems, we resort to solving them via SCA. The proposed iterative algorithm guarantees convergence to (at least) a locally optimal solution.

A. Binary Variable Relaxation

The relaxation of binary variables in (5e) and (5f) is carried out to circumvent the combinatorial nature of problem (5). The relaxed formulation for problem in (5) can be expressed as

$$\max_{\mathbf{W},\boldsymbol{\theta},\boldsymbol{\epsilon},\boldsymbol{\phi}} \quad \sum_{k\in\mathscr{K}} \phi_k \tag{6a}$$

$$\text{s. t.} \quad 0 \le \epsilon_{k,t} \le 1, \ \forall k \in \mathscr{K}, t \in \mathscr{T} \tag{6b}$$

$$0 \le \phi_k \le 1, \ \forall k \in \mathscr{K} \tag{6c}$$

$$(5b), (5c), (5d), (5g) \tag{6d}$$

where constraint (5e) and constraint (5f) are relaxed to box constraints between 0 and 1 in constraint (6b) and (6c), respectively. To guarantee that the values of $\epsilon_{k,t}$ and ϕ_k are equal to either one or zero, we consider additional constraints: $\epsilon_{k,t} - \epsilon_{k,t}^2 \le 0, \ \forall k,t$, which is equivalent to $\epsilon_{k,t} \in (-\infty, 0] \cup [1, +\infty), \ \forall k,t$ and $\phi_k - \phi_k^2 \le 0, \forall k$, which is equivalent to $\phi_k \in (-\infty, 0] \cup [1, +\infty), \forall k$. Therefore, $\epsilon_{k,t} - \epsilon_{k,t}^2 \le 0$ and (6b) hold true simultaneously only if $\epsilon_{k,t}$ is binary. Similarly, $\phi_k - \phi_k^2 \le 0$ and (6c) hold true only if ϕ_k is binary.

Accordingly, problem (6) can be transformed into the following form:

$$\max_{\mathbf{W},\boldsymbol{\theta},\boldsymbol{\epsilon},\boldsymbol{\phi}} \quad \sum_{k\in\mathscr{K}} \phi_k \tag{7a}$$

$$\text{s. t.} \quad 0 \le \epsilon_{k,t} \le 1, \quad \forall k \in \mathscr{K}, \ \forall t \in \mathscr{T} \tag{7b}$$

$$\epsilon_{k,t} - \epsilon_{k,t}^2 \le 0, \quad \forall k \in \mathscr{K}, \ \forall t \in \mathscr{T} \tag{7c}$$

$$0 \le \phi_k \le 1, \quad \forall k \in \mathscr{K} \tag{7d}$$

$$\phi_k - \phi_k^2 \le 0, \quad \forall k \in \mathscr{K} \tag{7e}$$

$$(5b), (5c), (5d), (5g). \tag{7f}$$

Remark 1: It is noted that constraints (7c) and (7e) usually make the problem (7) infeasible in most cases for $\epsilon_{k,t} \in (0,1)$ and $\phi_k \in (0,1)$, respectively. According to [48, Preposition 2], there exists a strong Lagrangian duality for the transformed problem (7). Following the same outlined procedure and similar mathematical formulations, we introduce two penalty functions as illustrated below. Specifically, we have exploited similar mathematical formulations in dealing with the binary nature of the problem. Accordingly, the inequalities in (7c) and (7e) are removed and their effects are modeled in the cost function.[4]

1) Penalty Functions: The two penalty functions are formulated as follows:

$$\begin{aligned}\mathcal{P}_1(\boldsymbol{\epsilon}, \mu_{\boldsymbol{\epsilon}}) &= \mu_{\boldsymbol{\epsilon}}\Big(\sum_{k\in\mathscr{K}}\sum_{t\in\mathscr{T}} \epsilon_{k,t}^2 - \sum_{k\in\mathscr{K}}\sum_{t\in\mathscr{T}} \epsilon_{k,t}\Big) \\ &\triangleq \mu_{\boldsymbol{\epsilon}}\big(h_1(\boldsymbol{\epsilon}) - g_1(\boldsymbol{\epsilon})\big)\end{aligned} \tag{8}$$

and

$$\begin{aligned}\mathcal{P}_2(\boldsymbol{\phi}, \mu_{\boldsymbol{\phi}}) &= \mu_{\boldsymbol{\phi}}\Big(\sum_{k\in\mathscr{K}} \phi_k^2 - \sum_{k\in\mathscr{K}} \phi_k\Big) \\ &\triangleq \mu_{\boldsymbol{\phi}}\big(h_2(\boldsymbol{\phi}) - g_2(\boldsymbol{\phi})\big).\end{aligned} \tag{9}$$

We note that the positive constants $\mu_{\boldsymbol{\epsilon}}$ and $\mu_{\boldsymbol{\phi}}$ in (8) and (9), respectively, are penalty parameters utilized to ensure the binary nature of the resulting binary matrix $\boldsymbol{\epsilon}$ and binary vector $\boldsymbol{\phi}$. By appropriately choosing the penalty parameters $\mu_{\boldsymbol{\epsilon}}$ and $\mu_{\boldsymbol{\phi}}$, the original problem can be solved.

Lemma 1: In the following, the relaxed problem in (7) is penalized with $\mathcal{P}_1(\boldsymbol{\epsilon}, \mu_{\boldsymbol{\epsilon}})$ and $\mathcal{P}_2(\boldsymbol{\phi}, \mu_{\boldsymbol{\phi}})$. Accordingly, we define the objective function to be minimized as $\psi(\boldsymbol{\epsilon}, \boldsymbol{\phi}) = -\sum_{k\in\mathscr{K}} \phi_k - \mu_{\boldsymbol{\epsilon}}\big(h_1(\boldsymbol{\epsilon}) - g_1(\boldsymbol{\epsilon})\big) - \mu_{\boldsymbol{\phi}}\big(h_2(\boldsymbol{\phi}) - g_2(\boldsymbol{\phi})\big)$. Given appropriate penalty parameters values $\mu_{\boldsymbol{\epsilon}}$ and $\mu_{\boldsymbol{\phi}}$, the problem in (7) (or the original problem (5)) and the following parameterized relaxed problem 10 become equivalent [48]:

$$\min_{\mathbf{W},\boldsymbol{\theta},\boldsymbol{\epsilon},\boldsymbol{\phi}} \quad \psi(\boldsymbol{\epsilon}, \boldsymbol{\phi}) \tag{10a}$$

$$\text{s. t.} \quad 0 \le \epsilon_{k,t} \le 1, \ \forall k \in \mathscr{K}, \forall t \in \mathscr{T} \tag{10b}$$

$$0 \le \phi_k \le 1, \forall k \in \mathscr{K} \tag{10c}$$

$$(5b), (5c), (5d), (5g). \tag{10d}$$

It is apparent that $h_1(\boldsymbol{\epsilon}) - g_1(\boldsymbol{\epsilon}) = 0$ and $h_2(\boldsymbol{\phi}) - g_2(\boldsymbol{\phi}) = 0$ must hold at optimum with appropriate values of $\mu_{\boldsymbol{\epsilon}}$ and $\mu_{\boldsymbol{\phi}}$, respectively; otherwise, $\mu_{\boldsymbol{\epsilon}}$ and $\mu_{\boldsymbol{\phi}}$ can be increased until the penalty values are close to zero. This implies that there always exists a positive penalty parameter $\mu_{\boldsymbol{\epsilon}}$ and $\mu_{\boldsymbol{\phi}}$ to obtain a solution. Further, $h_1(\boldsymbol{\epsilon})$ is always smaller than $g_1(\boldsymbol{\epsilon})$ for $\epsilon_{k,t}$ between 0 and 1. Also, the smallest difference between $h_1(\boldsymbol{\epsilon})$ and $g_1(\boldsymbol{\epsilon})$ is obtained with $\epsilon_{k,t} = 0$ or $\epsilon_{k,t} = 1$. Similarly, $h_1(\boldsymbol{\phi})$ is always smaller than $g_1(\boldsymbol{\phi})$ for ϕ_k values between 0 and 1. Unfortunately, the BS precoder and the phase shifts of the RIS are intricately coupled in the SINR constraint, making the parameterized relaxed problem in (10) non-convex and challenging to solve directly. More importantly, to make per-slot resource utilization more efficient, power should be allocated only to users that are considered served. In this case, we force $||\mathbf{w}_{k,t}||^2 = 0$ for all $\epsilon_{k,t} = 0$.[5] Next, we introduce a new variable $\boldsymbol{\varphi} \triangleq [\varphi_{k,t}]_{k\in\mathscr{K},T\in\mathscr{T}}$, where $\varphi_{k,t}$ is used to bound the sum interference power at user k in time slot t. Further, $\mathbf{h}_{k,t}$ denotes the normalized effective channel between the BS and the user k in time slot t, which is defined as $\mathbf{h}_{k,t} \triangleq (\mathbf{g}_{\mathsf{r}_{k,t}}\boldsymbol{\Theta}_t\mathbf{H}_t + \mathbf{g}_{\mathsf{d}_{k,t}})/\sigma$. We equivalently rewrite

[4]As we note in Remark 1, constraints (7c) and (7e) make problem (7) infeasible in most cases. Accordingly, we tackle the problem in (7e) by solving the relaxed version of the problem shown in (10). This is done by choosing the appropriate penalty functions, *i.e.* $\mathcal{P}_1(\boldsymbol{\epsilon}, \mu_{\boldsymbol{\epsilon}})$ and $\mathcal{P}_2(\boldsymbol{\phi}, \mu_{\boldsymbol{\phi}})$, which guarantees a (near)-exact binary solution at optimum.

[5]This can be formulated as $\sum_{k=1}^{K} \|\mathbf{w}_{k,t}\|^2 \epsilon_{k,t} \le P^{\max}$. However, the constraint is non-convex due to the strong coupling between $\mathbf{w}_{k,t}$ and $\epsilon_{k,t}$ which requires an approximation to convexify it. Accordingly, to convexify the constraint with less complexity, $\sum_{k=1}^{K} \|\mathbf{w}_{k,t}\|^2 \epsilon_{k,t} \le P^{\max}$ is replaced by constraint (11d) and (11e) which are both quadratic convex constraints.

problem (10) as

$$\min_{\mathbf{W},\boldsymbol{\theta},\boldsymbol{\epsilon},\boldsymbol{\phi},\boldsymbol{\varphi}} \ \psi(\boldsymbol{\epsilon},\boldsymbol{\phi}) \tag{11a}$$

$$\text{s. t.} \ \ \gamma_{\text{th}}\epsilon_{k,t} - \frac{|\mathbf{h}_{k,t}\mathbf{w}_{k,t}|^2}{\varphi_{k,t}} \le 0, \quad \forall k,t \tag{11b}$$

$$\sum_{i\in\mathscr{K}\setminus\{k\}} |\mathbf{h}_{k,t}\mathbf{w}_{i,t}|^2 + 1 \le \varphi_{k,t}, \quad \forall k,t \tag{11c}$$

$$\|\mathbf{w}_{k,t}\|^2 \le \epsilon_{k,t} P^{\max}, \quad \forall k, \ \forall t \tag{11d}$$

$$\sum_{k\in\mathscr{K}} \|\mathbf{w}_{k,t}\|^2 \le P^{\max}, \quad \forall t \tag{11e}$$

$$(5d), (5g), (10b), (10c). \tag{11f}$$

Remark 2: Note that constraint (11d) ensures that the beamforming vector for user k in time slot t is equal to zero when the user is not served. It can be seen that whenever $\epsilon_{k,t} = 0$, we have $\|\mathbf{w}_{k,t}\|^2 = 0$. Specifically, user k only needs to satisfy the QoS requirement, if it is served in time slot t.

The reformulated problem in (11) remains a non-convex problem even after binary variable relaxation. This is due to the objective (11a) and constraint (11b) which are non-convex. Accordingly, we propose an alternating optimization by splitting the problem into two tractable subproblems, which can be then solved effectively by SCA.

B. Proposed Alternating Optimization Algorithm Based on SCA

For an SCA-based iterative algorithm similar to [41], we denote by $(\mathbf{W}^{(\tau)}, \boldsymbol{\theta}^{(\tau)}, \boldsymbol{\epsilon}^{(\tau)}, \boldsymbol{\phi}^{(\tau)}, \boldsymbol{\varphi}^{(\tau)})$ the feasible point of (11) obtained in iteration τ. At iteration $\tau+1$, we solve problem (11) assuming a constant phase shift matrix $\boldsymbol{\theta}^{(\tau)}$, and then solve (11) assuming a constant precoding matrix $\mathbf{W}^{(\tau)}$. The two problems, *i.e.* precoding design and passive beamforming optimization are carried out alternatingly in each iteration.

1) Precoding Design: The precoding design problem is convexified in steps $12-18$ and its intermediate solution is found in Step 1 in Algorithm 1. The close-to-optimal solution of $\mathbf{w}^*_{k,t}$ is found after a finite number of iterations. At iteration $\tau+1$, we rewrite problem (11) for given $\boldsymbol{\theta}^{(\tau)}$ as

$$\mathscr{P}_{\mathbf{W}}: \min_{\mathbf{W},\boldsymbol{\epsilon},\boldsymbol{\phi},\boldsymbol{\varphi}} \ \psi(\boldsymbol{\epsilon},\boldsymbol{\phi}) \tag{12a}$$

$$\text{s. t.} \quad \gamma_{\text{th}}\epsilon_{k,t} - \frac{|\mathbf{h}_{k,t}\mathbf{w}_{k,t}|^2}{\varphi_{k,t}} \le 0, \quad \forall k,t \tag{12b}$$

$$(5g), (10b), (10c), (11c), (11d), (11e). \tag{12c}$$

We note that (12a) is non-convex and of type difference of convex (DC) functions. Also, constraint (12b) is non-convex. To convexify (12a), fortunately, we can approximate the convex functions $h_1(\boldsymbol{\epsilon}) \triangleq \sum_{k\in\mathscr{K}}\sum_{t\in\mathscr{T}} \epsilon^2_{k,t}$ and $h_2(\boldsymbol{\phi}) \triangleq \sum_{k\in\mathscr{K}} \phi_k^2$, which are quadratic. In this case, to approximate the two quadratic functions $h_1(\boldsymbol{\epsilon})$ and $h_2(\boldsymbol{\phi})$, we apply the first-order Taylor approximation to obtain a lower bound approximation around the feasible point $\boldsymbol{\epsilon}^{(\tau)}$ as

$$\begin{aligned} h_1(\boldsymbol{\epsilon}) &\ge h_1(\boldsymbol{\epsilon}^{(\tau)}) + \nabla_{\boldsymbol{\epsilon}} h_1(\boldsymbol{\epsilon}^{(\tau)})^T(\boldsymbol{\epsilon}-\boldsymbol{\epsilon}^{(\tau)}) \\ &= \sum_{k\in\mathscr{K}}\sum_{t\in\mathscr{T}} \Big(2\epsilon^{(\tau)}_{k,t}\epsilon_{k,t} - (\epsilon^{(\tau)}_{k,t})^2\Big) \triangleq h_1^{(\tau)}(\boldsymbol{\epsilon};\boldsymbol{\epsilon}^{(\tau)}) \end{aligned} \tag{13}$$

and around feasible point $\boldsymbol{\phi}^{(\tau)}$ as

$$\begin{aligned} h_2(\boldsymbol{\phi}) &\ge h_2(\boldsymbol{\phi}^{(\tau)}) + \nabla_{\boldsymbol{\phi}} h_2(\boldsymbol{\phi}^{(\tau)})^T(\boldsymbol{\phi}-\boldsymbol{\phi}^{(\tau)}) \\ &= \sum_{k\in\mathscr{K}} \Big(2\phi^{(\tau)}_{k}\phi_{k} - (\phi^{(\tau)}_{k})^2\Big) \triangleq h_2^{(\tau)}(\boldsymbol{\phi};\boldsymbol{\phi}^{(\tau)}) \end{aligned} \tag{14}$$

where $\nabla_{\boldsymbol{\epsilon}} h_1(\boldsymbol{\epsilon}) = 2\sum_{k\in\mathscr{K}}\sum_{t\in\mathscr{T}}\epsilon_{k,t}$ and $\nabla_{\boldsymbol{\phi}} h_2(\boldsymbol{\phi}) = 2\sum_{k\in\mathscr{K}}\boldsymbol{\phi}_k$. In this case, $h_1^{(\tau)}(\boldsymbol{\epsilon};\boldsymbol{\epsilon}^{(\tau)})$ and $h_2^{(\tau)}(\boldsymbol{\phi};\boldsymbol{\phi}^{(\tau)})$ are linear functions in $\boldsymbol{\epsilon}$ and $\boldsymbol{\phi}$, respectively. As a result, the objective (12a) is iteratively linearized as follows

$$\begin{aligned} \psi^{(\tau)}_{\mathbf{W}}(\boldsymbol{\epsilon},\boldsymbol{\phi}) \triangleq &-\sum_{k\in\mathscr{K}}\phi_k - \mu_{\boldsymbol{\epsilon}}\big(h_1^{(\tau)}(\boldsymbol{\epsilon};\boldsymbol{\epsilon}^{(\tau)}) - g_1(\boldsymbol{\epsilon})\big) \\ &- \mu_{\boldsymbol{\phi}}\big(h_2^{(\tau)}(\boldsymbol{\phi},\boldsymbol{\phi}^{(\tau)}) - g_2(\boldsymbol{\phi})\big). \end{aligned} \tag{15}$$

Further, we can note that function $\gamma_{k,t}(\mathbf{w}_{k,t},\varphi_{k,t}) \triangleq |\mathbf{h}_{k,t}\mathbf{w}_{k,t}|^2/\varphi_{k,t}$ in constraint (12b) is a quadratic-over-linear function. The global lower bound of $\gamma_k(\mathbf{w}_{k,t},\varphi_{k,t})$ around the feasible point $(\mathbf{w}^{(\tau)}_{k,t},\varphi^{(\tau)}_{k,t})$ is given by [49, Eq. (21)]:

$$\begin{aligned} &\gamma_k(\mathbf{w}_{k,t},\varphi_{k,t}) \\ &\ge \frac{2\,\text{Re}\Big\{(\mathbf{w}^{(\tau)}_{k,t})^H\mathbf{h}^H_{k,t}\mathbf{h}_{k,t}\mathbf{w}_{k,t}\Big\}}{\varphi^{(\tau)}_{k,t}} - \frac{|\mathbf{h}_{k,t}\mathbf{w}^{(\tau)}_{k,t}|^2}{(\varphi^{(\tau)}_{k,t})^2}\varphi_{k,t} \\ &\triangleq \gamma^{(\tau)}_{k,t}(\mathbf{w}_{k,t},\varphi_{k,t};\mathbf{w}^{(\tau)}_{k,t},\varphi^{(\tau)}_{k,t}). \end{aligned} \tag{16}$$

As a result, the constraint (12b) is replaced iteratively by the following convex constraint:

$$\gamma_{\text{th}}\epsilon_{k,t} - \gamma^{(\tau)}_{k,t}(\mathbf{w}_{k,t},\varphi_{k,t};\mathbf{w}^{(\tau)}_{k,t},\varphi^{(\tau)}_{k,t}) \le 0, \quad \forall k,t. \tag{17}$$

Accordingly, the convex precoding design solved at iteration $\tau+1$ is formulated as

$$\min_{\mathbf{W},\boldsymbol{\epsilon},\boldsymbol{\phi},\boldsymbol{\varphi}} \ \psi^{(\tau)}_{\mathbf{W}}(\boldsymbol{\epsilon},\boldsymbol{\phi}) \tag{18a}$$

$$\text{s. t.} \gamma_{\text{th}}\epsilon_{k,t} - \gamma^{(\tau)}_{k,t}(\mathbf{w}_{k,t},\varphi_{k,t};\mathbf{w}^{(\tau)}_{k,t},\varphi^{(\tau)}_{k,t}) \le 0, \quad \forall k,t \tag{18b}$$

$$(5g), (10b), (10c), (11c), (11d), (11e). \tag{18c}$$

a) Computation complexity: The problem (18) has $4KT+2K+T$ linear and quadratic constraints and $MKT+3KT+K$ decision variables. Accordingly, the worst-case computational complexity per iteration of solving (18) using interior point method is $\mathcal{O}\big(\sqrt{4KT+2K+T}(MKT+3KT+K)^3\big)$ [50, Chapter 6].

2) Passive Beamforming Design (or Phase Shift Optimization): At iteration $\tau+1$, problem (11) is rewritten for given $\mathbf{W}^{(\tau)}$ as

$$\mathscr{P}_{\boldsymbol{\theta}}: \min_{\boldsymbol{\theta},\boldsymbol{\epsilon},\boldsymbol{\phi},\boldsymbol{\varphi}} \ \psi(\boldsymbol{\epsilon},\boldsymbol{\phi}) \tag{19a}$$

$$\text{s. t.} \ \gamma_{\text{th}}\epsilon_{k,t} - \gamma_k(\boldsymbol{\theta}_t,\varphi_{k,t}) \le 0, \quad \forall k,t \tag{19b}$$

$$(5d), (5g), (10b), (10c), (11c) \tag{19c}$$

where $\gamma_{k,t}(\boldsymbol{\theta}_t, \varphi_{k,t}) \triangleq \dfrac{|(\mathbf{g}_{\mathsf{r}_{k,t}}\boldsymbol{\Theta}_t\mathbf{H}_t + \mathbf{g}_{\mathsf{d}_{k,t}})\mathbf{w}_{k,t}|^2}{\sigma^2\varphi_{k,t}}$. Here the objective function (19a) and constraint (19b) are non-convex. We observe that the convexification of objective function (19a) is already carried out in (15). Further, constraint (19b) can be approximated similarly to (18b). In particular, constraint (19b) is iteratively replaced by a convex constraint as follows:

$$\gamma_{\text{th}}\epsilon_{k,t} - \gamma_{k,t}^{(\tau)}(\boldsymbol{\theta}_t, \varphi_{k,t}; \boldsymbol{\theta}_t^{(\tau)}, \varphi_{k,t}^{(\tau)}) \leq 0, \ \forall k, t \tag{20}$$

where $\gamma_{k,t}^{(\tau)}(\boldsymbol{\theta}_t, \varphi_{k,t}; \boldsymbol{\theta}_t^{(\tau)}, \varphi_{k,t}^{(\tau)})$ is the global lower bound of $\gamma_{k,t}(\boldsymbol{\theta}_t, \varphi_{k,t})$, which is given as

$$\begin{aligned}
&\gamma_{k,t}^{(\tau)}(\boldsymbol{\theta}_t, \varphi_{k,t}; \boldsymbol{\theta}_t^{(\tau)}, \varphi_{k,t}^{(\tau)}) \\
&\triangleq \frac{2\,\text{Re}\left\{\mathbf{w}_{k,t}^H(\mathbf{g}_{\mathsf{r}_{k,t}}\boldsymbol{\Theta}_t^{(\tau)}\mathbf{H}_t + \mathbf{g}_{\mathsf{d}_{k,t}})^H(\mathbf{g}_{\mathsf{r}_{k,t}}\boldsymbol{\Theta}_t\mathbf{H}_t + \mathbf{g}_{\mathsf{d}_{k,t}})\mathbf{w}_{k,t}\right\}}{\sigma^2\varphi_{k,t}} \\
&\quad - \frac{|(\mathbf{g}_{\mathsf{r}_{k,t}}\boldsymbol{\Theta}_t^{(\tau)}\mathbf{H}_t + \mathbf{g}_{\mathsf{d}_{k,t}})\mathbf{w}_{k,t}|^2}{\left(\sigma\varphi_{k,t}^{(\tau)}\right)^2}\varphi_{k,t}.
\end{aligned} \tag{21}$$

The convex program of the passive beamforming design solved at iteration $\tau + 1$ is formulated as

$$\min_{\boldsymbol{\theta},\boldsymbol{\epsilon},\boldsymbol{\phi},\boldsymbol{\varphi}} \quad \psi_{\boldsymbol{\theta}}^{(\tau)}(\boldsymbol{\epsilon}, \boldsymbol{\phi}) \tag{22a}$$

$$\text{s. t. } \gamma_{\text{th}}\epsilon_{k,t} - \gamma_{k,t}^{(\tau)}(\boldsymbol{\theta}_t, \varphi_{k,t}; \boldsymbol{\theta}_t^{(\tau)}, \varphi_{k,t}^{(\tau)}) \leq 0, \quad \forall k, t \tag{22b}$$

$$(5d), (5g), (10b), (10c), (11c). \tag{22c}$$

a) Computation complexity: The problem in (22) has $2KT + 2K + NT + T$ linear and quadratic constraints and $NT + 2KT + K$ decision variables. Therefore, the computational complexity per iteration is $\mathcal{O}\big(\sqrt{2KT + 2K + NT + T}(NT + 2KT + K)^3\big)$.

The overall proposed iterative algorithm is summarized using pseudocode notation in Algorithm 1. The iterative procedure repeats until the fractional decrease in the value of the objective function for the overall problem is smaller than a predetermined threshold $\varrho = 10^{-3}$.

Algorithm 1 Proposed Alternating Optimization Algorithm

Input: Set $\tau = 1$ and initialized feasible points for $(\mathbf{W}^{(0)}, \boldsymbol{\theta}^{(0)}, \boldsymbol{\epsilon}^{(0)}, \boldsymbol{\phi}^{(0)}, \boldsymbol{\varphi}^{(0)})$ to constraints in (11)
repeat
Solve (18) for given $\boldsymbol{\theta}^{\tau}$ to obtain the optimal solutions $(\mathbf{W}^*, \boldsymbol{\epsilon}^*, \boldsymbol{\phi}^*, \boldsymbol{\varphi}^*)$;
Update $(\mathbf{W}^{(\tau+1)}, \boldsymbol{\epsilon}^{(\tau+1)}, \boldsymbol{\phi}^{(\tau+1)}, \boldsymbol{\varphi}^{(\tau+1)}) \triangleq (\mathbf{W}^*, \boldsymbol{\epsilon}^*, \boldsymbol{\phi}^*, \boldsymbol{\varphi}^*)$;
Solve (22) for given $(\mathbf{W}^{(\tau+1)}, \boldsymbol{\epsilon}^{(\tau+1)}, \boldsymbol{\phi}^{(\tau+1)}, \boldsymbol{\varphi}^{(\tau+1)}))$ to obtain the optimal solutions $(\boldsymbol{\theta}^*, \boldsymbol{\epsilon}^*, \boldsymbol{\phi}^*, \boldsymbol{\varphi}^*)$
Update $(\boldsymbol{\theta}^{(\tau+1)}, \boldsymbol{\epsilon}^{(\tau+1)}, \boldsymbol{\phi}^{(\tau+1)}, \boldsymbol{\varphi}^{(\tau+1)}) \triangleq (\boldsymbol{\theta}^*, \boldsymbol{\epsilon}^*, \boldsymbol{\phi}^*, \boldsymbol{\varphi}^*)$;
Set $\tau = \tau + 1$;
until the fractional decrease of the objective function is smaller than ϱ;
Output: $(\mathbf{W}^*, \boldsymbol{\theta}^*, \boldsymbol{\epsilon}^*, \boldsymbol{\phi}^*)$.

Initialization of feasible points: The proposed SCA-based AO algorithm requires initial feasible points to start at the first iterations, which are generated as follows. Firstly, $\boldsymbol{\epsilon}^{(0)}$ and $\boldsymbol{\phi}^{(0)}$ are randomly generated with respect to constraint 10b and 10c, respectively. Secondly, the phases of the RIS ($\boldsymbol{\theta}^{(0)}$) are randomly generated with respect to constraint 5d. For simplicity, the feasible point of $\mathbf{W}^{(0)}$ is obtained using a zero-forcing precoder. Accordingly, power allocation is carried out to satisfy the power budget. Finally, we generate $\varphi_{k,t}^{(o)}$ by setting $\varphi_{k,t}^{(o)} = \sum_{i\in\mathscr{K}\setminus\{k\}} |\mathbf{h}_{k,t}\mathbf{w}_{i,t}^{(0)}|^2 + 1, \forall k \in \mathscr{K}, \forall t \in \mathscr{T}$.

Penalty parameters selection μ_{ϵ} and μ_{ϕ}: The choice of an appropriate penalty parameter μ_{ϵ} and μ_{ϕ} is important for guaranteeing the performance/convergence of Algorithm 1 with reasonable computational time. In our simulations, we have numerically observed that $\mu_{\epsilon} = 0.0001$ and $\mu_{\phi} = 1$ are the most appropriate values that ensure that Algorithm 1 converges with exact binary solutions, while guaranteeing the best performance.

TABLE I
SIMULATION PARAMETERS

Simulation parameter	Value
Carrier frequency (f_c)	2.4 GHz
Noise power (σ^2)	-80 dBm
Per time slot SINR threshold (γ_{th})	10 dB
Minimum number of time slots to satisfy (α_{th})	5
Number of time slots (T)	10
Transmit power ($P^{\max}$)	20 dBm
BS height	3 m
UE height	1.5 m
RIS height	3 m
Minimum distance BS-user	30 m
Maximum distance BS-user	50 m
RIS dx distance	5 m
Pathloss exponent BS-RIS ($\zeta_{\text{bs-ris}}$)	2.3
Pathloss exponent RIS-user ($\zeta_{\text{ris-user}}$)	2.7
Pathloss exponent BS-user ($\zeta_{\text{bs-user}}$)	2.7
BS Antenna and RIS element spacing	0.5λ

V. NUMERICAL RESULTS

In this section, the performance of the proposed algorithm is evaluated against the benchmark schemes using Monte Carlo simulations. Following studies in [18], [51], [52], and [30], Table I provides the main simulation parameters. We assume that the location of the BS is at the origin and users are randomly distributed with uniform probability density between 30 m and 50 m in the y-axis. The RIS is deployed on a building facade, dx distance from the base station on the side of the street, see Fig 2. The RIS position in the y-direction can be varied. An independent Rician channel fading is considered for all the channels with the Rician factor β. For example, the BS-RIS channel $\mathbf{H}_t$ in time slot t is expressed as $\mathbf{H}_t = \sqrt{\frac{\beta}{1+\beta}}\mathbf{H}_t^{\text{LOS}} + \sqrt{\frac{1}{1+\beta}}\mathbf{H}_t^{\text{NLOS}}$. For $\beta = 0$, we would obtain a Rayleigh fading channel, whereas, for $\beta = \infty$, we would obtain a LoS propagation channel. Note that the RIS is typically deployed higher than the pedestrians in order to reduce the chance of signal blockage. Thus, less scattering environment is expected between the BS and the RIS, and thus, we set $\zeta_{\text{bs-ris}} < \zeta_{\text{bs-user}}$ [18]. The number of RIS elements is set at $N = 512$. In the following, Monte-Carlo simulations are carried out with 10^3 channel realizations for all the analyses in this paper.

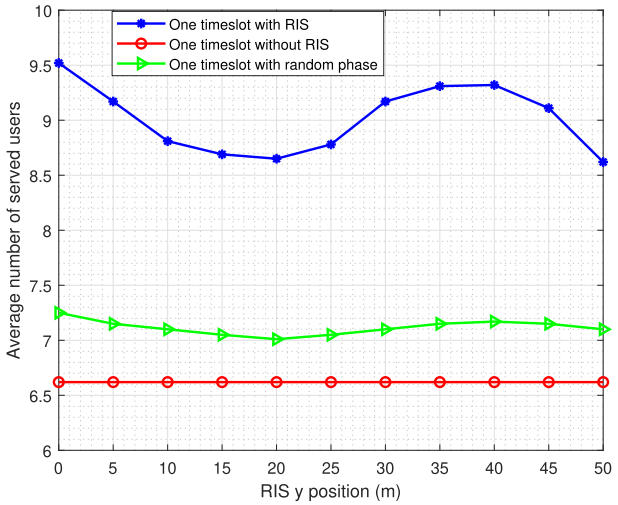

Fig. 4. Analysis of possible deployment positions for the RIS in the considered scenario.

A. Impact of RIS Deployment Position in the Proposed Scenario

A careful deployment of RIS is necessary to reach the maximum potential of RIS-aided networks. In this analysis, we compare the change in performance gain for different RIS deployment positions in the smart city street scenario. For simplicity, this analysis was carried out for joint precoding and passive beamforming design without scheduling. In this scenario, we set the number of BS antennas at $M = 10$ and the number of users $K = 10$. The Rician factor was set at $\beta = 3$ dB. Accordingly, we analyze the performance of joint precoding and passive beamforming design (One timeslot with RIS) with respect to different RIS positions, as shown in Fig. 4.

- **One timeslot without RIS**: The BS directly serves the users without taking the temporal dimension into account.
- **One timeslot with random phase**: The RIS phase shifts are not optimized, such that RIS represents a scatterer. In this case, while RIS has no capability of beamforming the signals toward users, it may still create additional signal paths which enhance the spatial diversity.

As illustrated in Fig. 4, we perform a line search to obtain the optimal RIS placement in the proposed scenario. We show performance as a function of RIS y position. We note that the performance of the proposed design varies with the RIS y position. By varying the RIS y position, we observe that the best performance in the proposed solution is obtained at RIS position $d = 0$ and $d = 40$ m in Fig. 4. This implies that a substantial reflection gain in the proposed scenario is obtained when the RIS is closest to the base station or in the middle of the segment where users are placed. Note that RIS position $d = 0$ does not imply that RIS is co-located with the base station since RIS is shifted by dx distance according to Fig. 2. Following this observation, we consider the BS side RIS deployment for all analyses in this work. Specifically, we choose the RIS deployment position that pertains to the highest number of served users, i.e. $d = 0$ m. The performance shows that the optimized reflection design performs better as compared to a random scatterer in the network. It is also important to note that even with the joint active and passive beamforming design (One timeslot with RIS), it is not possible to serve all users, especially if a large number of users demand access to the network. Accordingly, we analyze the necessity of joint scheduling, precoding, and passive beamforming design in the following subsections, especially when the network is overloaded.

B. Benchmark Schemes

The proposed joint multislot scheduling, precoding and passive beamforming design (JSP with RIS) is compared with the following three baseline schemes to better analyze its performance gain:

- Joint multislot scheduling, precoding and passive beamforming without RIS (JSP without RIS): No RIS is assumed in the system. The joint multislot scheduling and precoding is designed with users served directly by the BS. The penalty parameters are set to $\mu_{\boldsymbol{\epsilon}} = 0.0001$ and $\mu_{\boldsymbol{\phi}} = 1$.
- Joint precoding and passive beamforming (one-time slot): Users are served by a RIS-aided network continuously without multislot scheduling. The penalty parameter for this scheme is set to $\mu_{\text{Onetimeslot}} = 0.2$ [1].
- Joint precoding and passive beamforming with reduced SINR threshold (SINR adaptation): While the QoS per time slot may be the same with the proposed solution (JSP with RIS) and the benchmark scheme without scheduling (one-time slot), the average data rate of the served users may not be the same (the average rate is lower, if the user is served in just a few time slots) as with continuous transmissions. For a fair comparison, in this benchmark scheme, we maximize the number of served users, for which the minimum data rate with a continuous transmission is the same as the average (over the time window) data rate of the proposed solution. For this, we perform SINR adaptation, *i.e.* we reduce the SINR threshold to match the two data rates. We solve $\frac{\alpha_{\text{th}}}{T}\log_2(1+\gamma_{\text{th}}) = \log_2(1+\gamma_{\text{th,adapt}})$ with respect to $\gamma_{\text{th,adapt}}$, where $\gamma_{\text{th,adapt}}$ is the new SINR threshold. In this case, for $\gamma_{\text{th}} = 10$ dB, $\alpha_{\text{th}} = 5$ and $T = 10$, $\gamma_{\text{th,adapt}} = 3.6$ dB. The penalty parameter for this scheme is set to $\mu_{\text{adapt}} = 0.2$.

C. Convergence Analysis

Here, we show the convergence of all the considered schemes. For this analysis, we fix the number of users at $K = 12$, the number of BS antennas at $M = 6$ and the Rician factor at $\beta = 3$ dB. As can be observed from Fig. 5, all the considered schemes converge quickly to the stationary point within about 11 iterations. In addition, the objective values are non-decreasing after each iteration, satisfying the inner approximation properties, thus proving that the algorithm indeed converges to a local optimum [41], [53]. Another interesting observation is that the one timeslot and SINR adaptation schemes converge faster than other ones, but provide a much lower number of users served. This is attributed to the fact that these two schemes do not jointly optimize

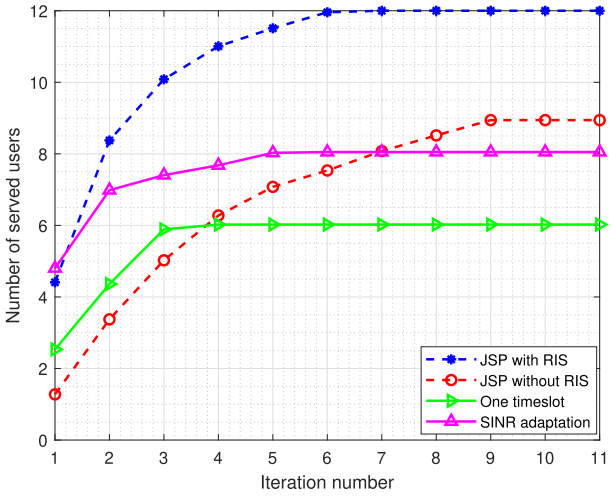

Fig. 5. Convergence behavior of all the considered schemes.

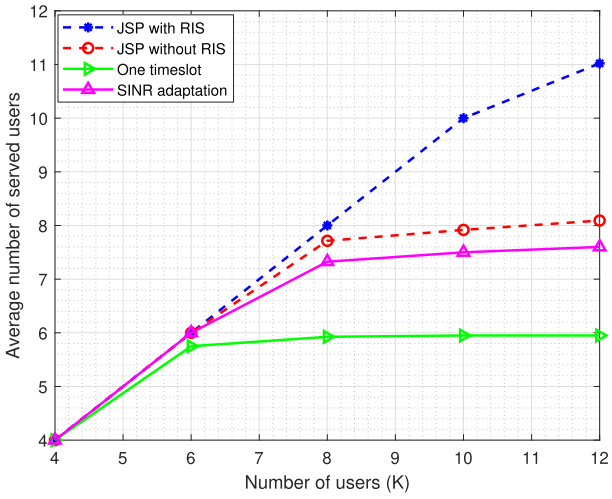

Fig. 6. Average number of served users as a function of the total number of users (K) demanding access to the network.

the scheduling, resulting in faster convergence but less time diversity to serve all users. Nevertheless, the proposed scheme offers the best performance in terms of the number of served users, confirming the effectiveness of the joint optimization of multislot scheduling, precoding and passive beamforming.

D. Analysis of Average Number of Served Users Versus Total Number of Users

In this subsection, we analyze the average number of served users as a function of the total number of users K demanding access to the network. We set the number of BS transmit antennas $M = 6$ and the total number of users is varied from $K = 4$ to $K = 12$ in steps of 2. The Rician factor is set at $\beta = 3$ dB. The results are depicted in Fig. 6. It can be noted that when the number of users is low, the JSP with RIS (Proposed solution) cannot provide significant gain since the available diversity is sufficient to serve all users even without scheduling. However, we can observe an increase in the gain of the JSP with RIS scheme starting from $K = 6$. This proves the necessity of scheduling, especially in an overloaded network, where $K > M$. The JSP with RIS manages to serve all users

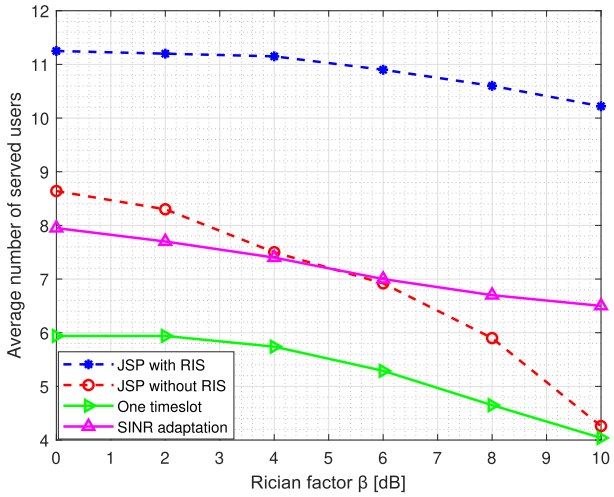

Fig. 7. Average number of served users as a function of the Rician factor (β) in dB.

up to $K = 10$, whereas the other two benchmark schemes (the JSP without RIS and the SINR adaptation) only manage to serve all users until $K = 6$, which is equal to M. Moreover, the one-time slot benchmark converges to $M = 6$ as this is the maximum number of orthogonal links in this system. Further, we can note that the JSP without RIS scheme converges to a larger number of users than the schemes with RIS but without scheduling (even in the case of SINR adaptation) due to the time diversity, which provides more degrees of freedom than the spatial diversity provided by the joint precoding and passive beamforming without scheduling. An important observation is that with SINR adaptation, we manage to serve more than $M = 6$ users even without scheduling, since the SINR threshold is much lower than the target SINR of other benchmarks, *i.e.* we can tolerate much more interference and the channels do not need to be close to orthogonal. In this case, the RIS helps to filter the signal and reduce interference. The benchmark JSP without RIS results in an increased probability to serve more users as the total number of users increases, however, its performance starts to converge at $K = 8$ since it does not have an additional degree of freedom provided by RIS deployment in the network.

E. Analysis of Served Users With Varying Rician Factor

In this subsection, we evaluate how the Rician factor β affects the performance of the considered design methods.

The Rician factor β is varied from 0 dB to 10 dB in steps of 2 dB. We set the total number of BS antennas at $M = 6$ and the total number of users requesting access to the network at $K = 12$. As observed in Fig. 7, RIS-aided communication curves exhibit similar behavior in terms of performance degradation with increasing Rician factor. This behavior is different without RIS, *i.e.* the degradation is much faster and steeper. The reason is that RIS substantially enhances the spatial diversity of the system, such that the reduction of the spatial diversity with respect to the BS can be partially compensated by the RIS. The results shown in Fig. 7 indicate that JSP with RIS leads to a substantial increase in the average

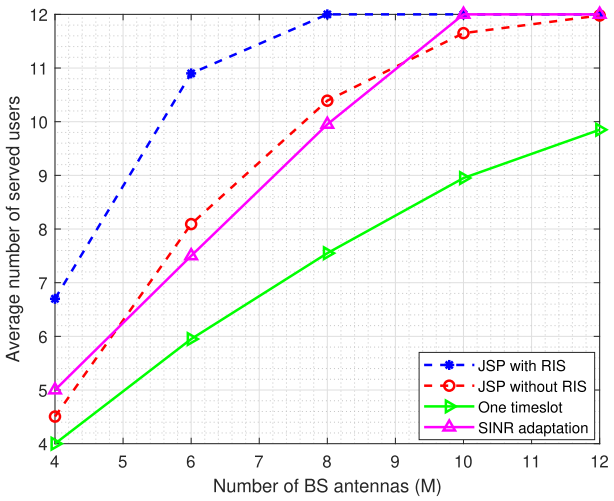

Fig. 8. Average number of served users as a function of the total number of BS antennas (M).

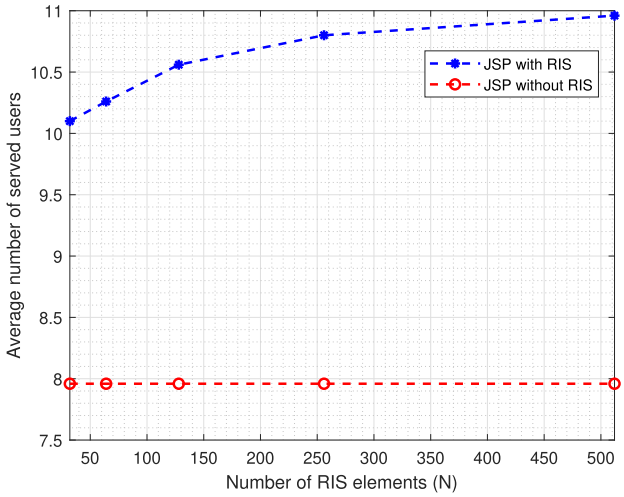

Fig. 9. Average number of served users with an increasing number of elements.

number of users served as compared to the three benchmark schemes. However, we observe that the average number of served users for the considered schemes decreases with the increasing Rician factor. Due to the unlucky distribution of users on the street with respect to the BS (*i.e.* the limited angular spread), for a pure LoS propagation, it may not be possible to serve more than 1 user as a result of a very high degree of correlation between the channels. The performance of the considered schemes degrades as the diversity reduces, *i.e.* the channel becomes a pure LoS propagation channel. In this case, the available diversity is not sufficient to produce independent beams with acceptable signal quality. However, the JSP with RIS scheme can still serve a significant number of users with increasing Rician factor as compared to the scheme without RIS. In this case, we note a difference of at least 5 more users on average as compared to the benchmark without RIS at $\beta = 10$ dB.

F. Analysis of Served Users With Varying Total Number of BS Antennas

In this subsection, we vary the number of BS antennas from $M = 4$ to $M = 12$ in steps of 2. The number of users is fixed at $K = 12$ and the Rician factor $\beta = 3$ dB. The results are depicted in Fig. 8.

It is important to note that the JSP with RIS design is very beneficial in this setup especially when the number of users K is much larger than the number of antennas M at the BS. At $M = 4$, the JSP with RIS outperforms the benchmark scheme without RIS by at least 2 additional users. In fact, $M = 8$ is enough for the proposed method to serve all users. Further, we can note that as the number of antennas M approaches the number of users K, the JSP with RIS does not provide a significant gain since the available multiplexing capability brought by the antennas is enough for the SINR adaptation and the JSP without RIS to serve all users. An important observation is that the highest gain of the JSP with RIS is recorded when the number of users K is double the number of BS antennas M. We can note that $K = 12$ corresponds to the maximum number of users. In this case, with an increasing number of BS antennas, the diversity degree increases, such that more and more users can be served. Therefore, all curves converge to the maximum number K with an increasing number of antennas. It seems that for most of the curves (except one-time slot) there is enough diversity already with $M = 12$ transmit antennas, which is due to a combination of time diversity and spatial diversity. In the case of one-time slot, we only have spatial diversity, which is not sufficient, which is why we would need more transmit antennas to serve the maximum number of users.

G. Impact of the Number of RIS Elements

In this subsection, we investigate the impact of the number of RIS elements on the system performance. We set the total number of BS antennas at $M = 6$, the total number of users requesting access to the network at $K = 12$ and the Rician factor β is set at 3 dB. We varied the number of RIS elements from $N = 32$ to $N = 512$. In this investigation, the proposed design (JSP with RIS) was compared to the benchmark scheme without RIS (JSP without RIS). As shown in Fig. 9, the proposed design provides a significant performance improvement as compared to the considered benchmark scheme. The gain provided by the proposed design increases with the increasing number of RIS elements. Specifically, simulation results demonstrate a notable increase in the average number of users served as the number of RIS elements increases. This validates the benefit of RIS deployment in the considered scenario for an improved spatial multiplexing gain.

H. Impact of RIS Deployment Height

In this subsection, we investigate the impact of the RIS height on the system performance. To gain more insights into the impact of the RIS deployment height on the system performance, we evaluate the average number of served users as a function of RIS deployment position for different RIS deployment heights. Note that this analysis is carried out for a one-time slot scheme for simplicity. The number of BS

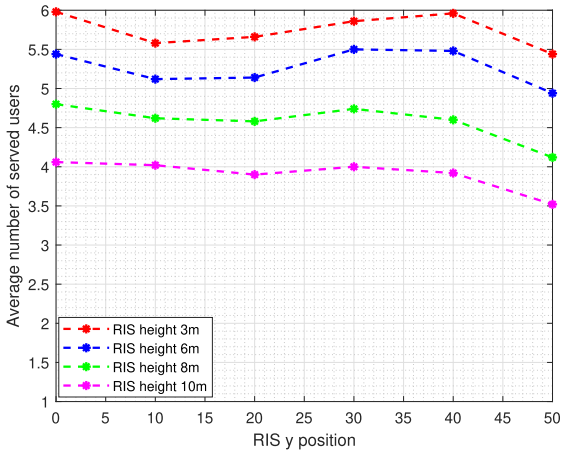

(a) BS height 3 m

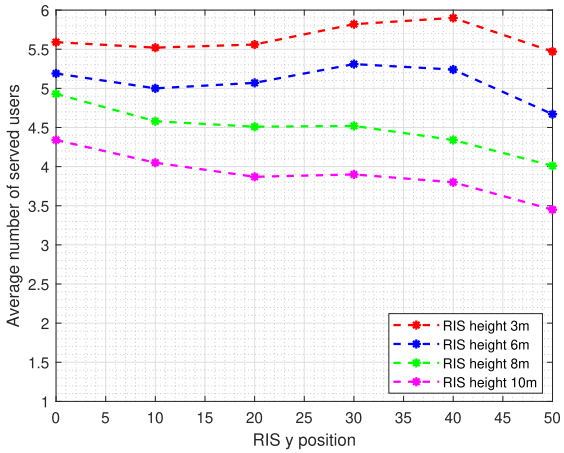

(b) BS height 10 m

Fig. 10. Impact of RIS deployment height.

antennas is fixed to $M = 6$ and the number of users is $K = 12$. We investigate the performance for BS height of 3 m and 10 m as shown in Figs. 10(a) and 10(b), respectively. The height of the RIS is varied between $3 - 10$ m and the user height is fixed at 1.5 m. We gradually increase the Rician factor in proportion to the different RIS heights in order to account for the reducing number of obstacles with increasing deployment height, which generate additional non-LoS paths [54]. In Fig. 10(a), we investigate the performance for different heights of the RIS with the BS height fixed at 3 m. We assume that the BS in this scenario is deployed on street infrastructure which includes light poles, bus station enclosures, streetlights, and utility poles. As previously discussed, better performance gain is observed when the RIS is deployed closer to the base station (BS-side deployment) or closer to users (user-side deployment). Here, we can see that the system performance is improved when the RIS's height is about 3 m. We also show that the best performance in this system setup is obtained when the RIS deployment height is similar to the BS's height. In Fig. 10(b), we set the BS height at 10 m. We investigate the performance for different heights of the RIS. It is important to note that increasing RIS height decreases the number of served users. In this setup, we observe the highest gain at RIS height 3 m. However, we can see that the best performance is

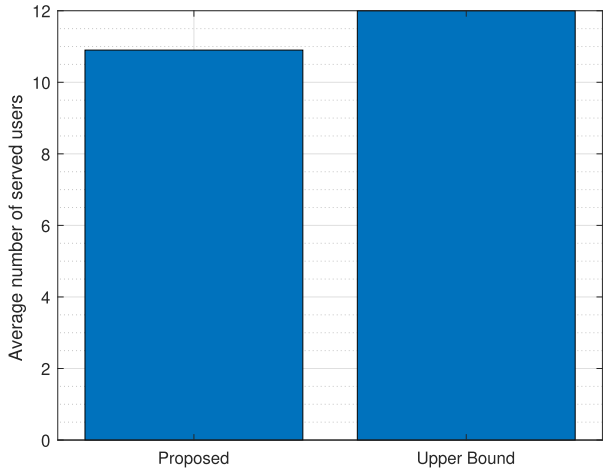

Fig. 11. Comparison with the Upper Bound.

when the RIS is deployed close to users. This is because the RIS height is close to the height of the users which is fixed at 1.5 m. Accordingly, an important observation is that for all RIS heights, the performance of BS-side deployment is more significant if the RIS deployment height is closer or similar to the BS height. Further, the performance of the user-side deployment is significant if the RIS height is closer or similar to the user deployment height. As a result, to obtain better gain, RIS deployment height should be similar to the height of the closest node, i.e. similar to BS height if near BS or similar to user height if near users.

I. Comparison With an Upper Bound

In this subsection, we compare our proposed design with an upper-bound solution. Note that the formulated problem is a mixed-integer nonlinear program (MINLP) which is non-convex and thus difficult to solve in polynomial time using existing methods of combinatorial programming and convex optimization. Such non-convex problems have no established standard approach for solving them optimally, making it challenging to find an existing algorithm that can efficiently provide an optimal solution. However, in order to evaluate the tightness of the proposed algorithm to the theoretical limit, we compare the proposed algorithm with an upper-bound solution. Specifically, we derive the upper bound on the number of users that the system can support considering the number of packets required for the user to be considered served and the maximum number of orthogonal channels we can create in each time slot. Accordingly, we can estimate theoretically the number of users that can be served. The maximum number of users that the system can support is

$$K_{\text{tot}} = \frac{MT}{\alpha_{\text{th}}} \tag{23}$$

where T is the number of timeslots, M is the number of BS antennas, and α_{th} is the minimum number of time slots required to meet the QoS requirements. Accordingly, we demonstrate the performance of the proposed algorithm as compared to the upper-bound solution as shown in Fig. 11.

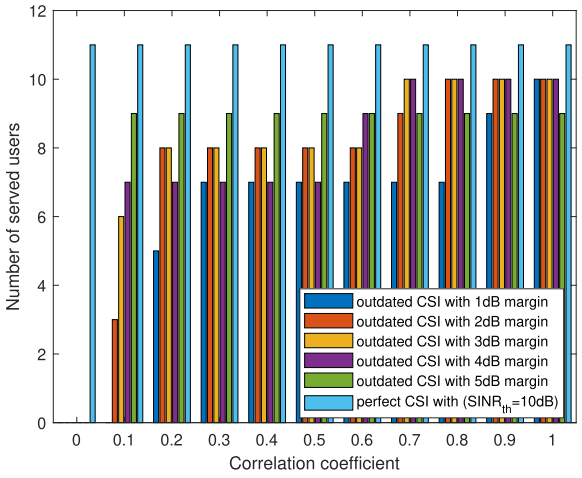

Fig. 12. Impact of outdated CSI with different QoS margins.

J. Impact of Outdated CSI on the System Performance

In this subsection, we investigate the impact of outdated CSI on the system performance in high mobility scenarios. We note that when the CSI becomes more and more outdated, it becomes very challenging to serve users with the desired QoS. Accordingly, we propose a QoS margin to improve the system's robustness to outdated CSI. Firstly, we assume that the channel from the BS to the RIS can be estimated perfectly since the position of the BS and the RIS is fixed. Due to the mobility of users, the BS to user and RIS to user channels may often be outdated. Accordingly, we denote the BS to user k link in time slot t, by $\mathbf{g}^0_{\mathrm{d}_{k,t}}$ and the RIS to user k channel in time slot t by $\mathbf{g}^0_{\mathrm{r}_{k,t}}$. Specifically, the true channels from BS to user k and RIS to user k in time slot t, can be expressed,respectively, as [55]:

$$\mathbf{g}^0_{\mathrm{d}_{k,t}} = \varrho \mathbf{g}_{\mathrm{d}_{k,t}} + \sqrt{1-\varrho^2}\varepsilon \tag{24}$$

$$\mathbf{g}^0_{\mathrm{r}_{k,t}} = \varrho \mathbf{g}_{\mathrm{r}_{k,t}} + \sqrt{1-\varrho^2}\varepsilon \tag{25}$$

where $\mathbf{g}_{\mathrm{d}_{k,t}}$ and $\mathbf{g}_{\mathrm{r}_{k,t}}$ are the outdated estimated channels for user k in time slot t. Herein, $0 \leq \varrho \leq 1$ is the correlation coefficient between the estimated channel that is outdated and the true channel. Further, ε is a complex Gaussian distribution with zero mean and variance σ^2. The estimate channels are modeled as described in the previous section, following a Rician fading model. We note that when $\varrho = 1$, the CSI is considered to be perfectly available at the transmitter, whereas $\varrho = 0$ denotes the unavailability of CSI. According to [56], the correlation coefficient ϱ can be calculated as follows

$$\varrho = J_0\left(\frac{2\pi f_c v T_e}{c}\right) \tag{26}$$

where f_c is the carrier frequency, v is the user velocity, T_e is the estimation delay between the outdated channel estimate and the true channel and $J_0(.)$ is the zeroth-order Bessel function of the first order. To reduce the impact of outdated CSI on the performance of the overall algorithm, we introduce a quality of service margin. Specifically, we consider the SINR margin of $1-5$ dB. This is to ensure the robustness of the proposed approach to the impact of outdated CSI. In this case, we can still be able to provide users with a QoS threshold of 10 dB. As illustrated in Fig. 12, we note that the number of served users decreases as the correlation coefficient ϱ decreases. Specifically, the number of users served reduces as the channel becomes more and more outdated. However, we observed that, varying the QoS margin between 1 dB to 5 dB margin can help minimize the impact of outdated CSI on the overall system performance. This confirms the robustness provided by the introduction of the QoS margin to reduce the effect of outdated CSI for different correlation coefficients. It is also important to note that a 5 dB margin provides a more robust solution when the correlation coefficient is small. However, it is outperformed by other margins when the correlation coefficient is larger than 0.6.

It is evident from the results that the joint multislot scheduling, precoding and passive beamforming design leads to substantial performance gains, especially in an overloaded network where the number of BS antennas is less than the number of users. This gain highly depends on several system parameters such as the RIS deployment position, number of RIS elements, Rician factor, the total number of users on the street, number of BS antennas, user QoS requirements, and quality of CSI. Further, the deployment of RIS in this scenario has quite a huge impact on improving the network's multiplexing capabilities.

VI. Conclusion

In this paper, we studied the joint optimization of scheduling, precoding and passive beamforming for a RIS-aided network in a realistic smart city scenario. Specifically, the multislot scheduling, precoding at the BS and passive beamforming at the RIS are jointly optimized to maximize the admission of users, *i.e.*, the number of served users in a challenging smart city street while satisfying QoS targets. The formulated problem is mixed-integer nonlinear programming, which is NP-hard. Combining tools from binary variable relaxation, alternating optimization and successive convex approximations, we developed an efficient iterative algorithm to solve the problem. Interestingly, it is shown that the proposed method is more applicable in an overloaded network as compared to the design without scheduling. Further, taking advantage of the spatial diversity enhancement provided by RIS deployment and the time diversity from scheduling, we observed a significant performance gain compared to all the considered benchmark schemes. Simulation results showed a notable performance improvement in terms of the number of served users, which is quite beneficial for the target application *i.e.* smart city, where there is a proliferation of devices demanding access to the network. Simulation results have also illustrated that in case of outdated CSI due to user mobility, the introduction of a QoS margin improves the robustness of the proposed algorithm.

References

[1] P. Zivuku et al., "Maximizing the number of served users in a smart city using reconfigurable intelligent surfaces," in *Proc. IEEE Wireless Commun. Netw. Conf. (WCNC)*, Apr. 2022, pp. 494–499.

[2] I. Yildirim, A. Uyrus, and E. Basar, "Modeling and analysis of reconfigurable intelligent surfaces for indoor and outdoor applications in future wireless networks," *IEEE Trans. Commun.*, vol. 69, no. 2, pp. 1290–1301, Feb. 2021.

[3] M. D. Renzo et al., "Smart radio environments empowered by reconfigurable AI meta-surfaces: An idea whose time has come," *EURASIP J. Wireless Commun. Netw.*, vol. 2019, no. 1, pp. 1–20, Dec. 2019.

[4] Q. Wu and R. Zhang, "Towards smart and reconfigurable environment: Intelligent reflecting surface aided wireless network," *IEEE Commun. Mag.*, vol. 58, no. 1, pp. 106–112, Jan. 2020.

[5] W. Mei and R. Zhang, "Performance analysis and user association optimization for wireless network aided by multiple intelligent reflecting surfaces," *IEEE Trans. Commun.*, vol. 69, no. 9, pp. 6296–6312, Sep. 2021.

[6] M. Di Renzo et al., "Reconfigurable intelligent surfaces vs. relaying: Differences, similarities, and performance comparison," *IEEE Open J. Commun. Soc.*, vol. 1, pp. 798–807, 2020.

[7] C. Pan et al., "An overview of signal processing techniques for RIS/IRS-aided wireless systems," 2021, *arXiv:2112.05989*.

[8] E. Björnson, H. Wymeersch, B. Matthiesen, P. Popovski, L. Sanguinetti, and E. de Carvalho, "Reconfigurable intelligent surfaces: A signal processing perspective with wireless applications," *IEEE Signal Process. Mag.*, vol. 39, no. 2, pp. 135–158, Mar. 2022.

[9] E. Basar, M. Di Renzo, J. De Rosny, M. Debbah, M.-S. Alouini, and R. Zhang, "Wireless communications through reconfigurable intelligent surfaces," *IEEE Access*, vol. 7, pp. 116753–116773, 2019.

[10] S. Dirks and M. Keeling, "A vision of smarter cities: How cities can lead the way into a prosperous and sustainable future," IBM Inst. Bus. Value, 2009, p. 8.

[11] B. N. Silva, M. Khan, and K. Han, "Towards sustainable smart cities: A review of trends, architectures, components, and open challenges in smart cities," *Sustain. Cities Soc.*, vol. 38, pp. 697–713, Apr. 2018.

[12] S. Kisseleff, W. A. Martins, H. Al-Hraishawi, S. Chatzinotas, and B. Ottersten, "Reconfigurable intelligent surfaces for smart cities: Research challenges and opportunities," *IEEE Open J. Commun. Soc.*, vol. 1, pp. 1781–1797, 2020.

[13] M. Di Renzo et al., "Smart radio environments empowered by reconfigurable intelligent surfaces: How it works, state of research, and the road ahead," *IEEE J. Sel. Areas Commun.*, vol. 38, no. 11, pp. 2450–2525, Nov. 2020.

[14] T. Zhang, H. Wen, Z. Pang, and H. Song, "CSI-free physical layer security against eavesdropping attack based on intelligent surface for industrial wireless," in *Proc. 17th IEEE Int. Conf. Factory Commun. Syst. (WFCS)*, Jun. 2021, pp. 175–182.

[15] J. Zhang, H. Du, Q. Sun, B. Ai, and D. W. K. Ng, "Physical layer security enhancement with reconfigurable intelligent surface-aided networks," *IEEE Trans. Inf. Forensics Security*, vol. 16, pp. 3480–3495, 2021.

[16] M. H. Khoshafa, T. M. N. Ngatched, and M. H. Ahmed, "Reconfigurable intelligent surfaces-aided physical layer security enhancement in D2D underlay communications," *IEEE Commun. Lett.*, vol. 25, no. 5, pp. 1443–1447, May 2021.

[17] J. Luo, F. Wang, S. Wang, H. Wang, and D. Wang, "Reconfigurable intelligent surface: Reflection design against passive eavesdropping," *IEEE Trans. Wireless Commun.*, vol. 20, no. 5, pp. 3350–3364, May 2021.

[18] X. Guan, Q. Wu, and R. Zhang, "Intelligent reflecting surface assisted secrecy communication: Is artificial noise helpful or not?" *IEEE Wireless Commun. Lett.*, vol. 9, no. 6, pp. 778–782, Jun. 2020.

[19] D. Xu, X. Yu, Y. Sun, D. W. K. Ng, and R. Schober, "Resource allocation for secure IRS-assisted multiuser MISO systems," in *Proc. IEEE Globecom Workshops*, Dec. 2019, pp. 1–6.

[20] P. Wang, J. Fang, X. Yuan, Z. Chen, and H. Li, "Intelligent reflecting surface-assisted millimeter wave communications: Joint active and passive precoding design," *IEEE Trans. Veh. Technol.*, vol. 69, no. 12, pp. 14960–14973, Dec. 2020.

[21] D. Xu, X. Yu, Y. Sun, D. W. K. Ng, and R. Schober, "Resource allocation for IRS-assisted full-duplex cognitive radio systems," *IEEE Trans. Commun.*, vol. 68, no. 12, pp. 7376–7394, Dec. 2020.

[22] Q. Wu and R. Zhang, "Beamforming optimization for wireless network aided by intelligent reflecting surface with discrete phase shifts," *IEEE Trans. Commun.*, vol. 68, no. 3, pp. 1838–1851, Mar. 2020.

[23] Z. Yang, W. Xu, C. Huang, J. Shi, and M. Shikh-Bahaei, "Beamforming design for multiuser transmission through reconfigurable intelligent surface," *IEEE Trans. Commun.*, vol. 69, no. 1, pp. 589–601, Jan. 2021.

[24] Q. Wu and R. Zhang, "Intelligent reflecting surface enhanced wireless network: Joint active and passive beamforming design," in *Proc. IEEE Global Commun. Conf.*, Dec. 2018, pp. 1–6.

[25] Y. Cai, M.-M. Zhao, K. Xu, and R. Zhang, "Intelligent reflecting surface aided full-duplex communication: Passive beamforming and deployment design," *IEEE Trans. Wireless Commun.*, vol. 21, no. 1, pp. 383–397, Jan. 2022.

[26] Q.-U.-A. Nadeem, A. Kammoun, A. Chaaban, M. Debbah, and M.-S. Alouini, "Asymptotic max-min SINR analysis of reconfigurable intelligent surface assisted MISO systems," *IEEE Trans. Wireless Commun.*, vol. 19, no. 12, pp. 7748–7764, Dec. 2020.

[27] J. Li and J. Liu, "Sum rate maximization via reconfigurable intelligent surface in UAV communication: Phase shift and trajectory optimization," in *Proc. IEEE/CIC Int. Conf. Commun. China*, Mar. 2020, pp. 124–129.

[28] Y. Cao and T. Lv, "Sum rate maximization for reconfigurable intelligent surface assisted device-to-device communications," 2020, *arXiv:2001.03344*.

[29] N. S. Perović, L. N. Tran, M. Di Renzo, and M. F. Flanagan, "Achievable rate optimization for MIMO systems with reconfigurable intelligent surfaces," *IEEE Trans. Wireless Commun.*, vol. 20, no. 6, pp. 3865–3882, Jun. 2021.

[30] Ö. Özdogan, E. Björnson, and E. G. Larsson, "Using intelligent reflecting surfaces for rank improvement in MIMO communications," in *Proc. IEEE Int. Conf. Acoust., Speech Signal Process. (ICASSP)*, May 2020, pp. 9160–9164.

[31] A. Bandi, B. Shankar, S. Chatzinotas, and B. Ottersten, "A joint solution for scheduling and precoding in multiuser MISO downlink channels," *IEEE Trans. Wireless Commun.*, vol. 19, no. 1, pp. 475–490, Jan. 2020.

[32] J. Lin, M. Ma, Q. Li, and J. Yang, "Joint long-term admission control and beamforming in green downlink networks: Offline and online approaches," *IEEE Trans. Veh. Technol.*, vol. 69, no. 8, pp. 8710–8724, Aug. 2020.

[33] K. B. S. Manosha, S. K. Joshi, M. Codreanu, N. Rajatheva, and M. Latva-aho, "Admission control algorithms for QoS-constrained multicell MISO downlink systems," *IEEE Trans. Wireless Commun.*, vol. 17, no. 3, pp. 1982–1999, Mar. 2018.

[34] R. S. Chaves, M. V. S. Lima, E. Cetin, and W. A. Martins, "User selection for massive MIMO under line-of-sight propagation," *IEEE Open J. Commun. Soc.*, vol. 3, pp. 867–887, 2022.

[35] S. He, J. Yuan, Z. An, Y. Yi, and Y. Huang, "Maximizing the set cardinality of users scheduled for ultra-dense uRLLC networks," *IEEE Commun. Lett.*, vol. 25, no. 12, pp. 3952–3955, Dec. 2021.

[36] A. Bandi, M. R. B. Shankar, S. Chatzinotas, and B. Ottersten, "Joint multislot scheduling and precoding for unicast and multicast scenarios in multiuser MISO systems," *IEEE Trans. Wireless Commun.*, vol. 21, no. 7, pp. 5004–5018, Jul. 2022.

[37] Z. Zhang, T. Jiang, and W. Yu, "User scheduling using graph neural networks for reconfigurable intelligent surface assisted multiuser downlink communications," in *Proc. IEEE Int. Conf. Acoust., Speech Signal Process. (ICASSP)*, May 2022, pp. 8892–8896.

[38] A. Al-Hilo, M. Samir, M. Elhattab, C. Assi, and S. Sharafeddine, "Reconfigurable intelligent surface enabled vehicular communication: Joint user scheduling and passive beamforming," *IEEE Trans. Veh. Technol.*, vol. 71, no. 3, pp. 2333–2345, Mar. 2022.

[39] Z. Zhang, T. Jiang, and W. Yu, "Learning based user scheduling in reconfigurable intelligent surface assisted multiuser downlink," *IEEE J. Sel. Topics Signal Process.*, vol. 16, no. 5, pp. 1026–1039, Aug. 2022.

[40] E. Matskani, N. Sidiropoulos, Z.-Q. Luo, and L. Tassiulas, "Convex approximation techniques for joint multiuser downlink beamforming and admission control," *IEEE Trans. Wireless Commun.*, vol. 7, no. 7, pp. 2682–2693, Jul. 2008.

[41] A. Beck, A. Ben-Tal, and L. Tetruashvili, "A sequential parametric convex approximation method with applications to nonconvex truss topology design problems," *J. Global Optim.*, vol. 47, no. 1, pp. 29–51, May 2010.

[42] H. Guo, Y.-C. Liang, J. Chen, and E. G. Larsson, "Weighted sum-rate maximization for intelligent reflecting surface enhanced wireless networks," in *Proc. IEEE Global Commun. Conf. (GLOBECOM)*, Dec. 2019, pp. 1–6.

[43] M. Cui, G. Zhang, and R. Zhang, "Secure wireless communication via intelligent reflecting surface," *IEEE Wireless Commun. Lett.*, vol. 8, no. 5, pp. 1410–1414, Oct. 2019.

[44] J. Zheng, J. Zhang, E. Björnson, and B. Ai, "Impact of channel aging on cell-free massive MIMO over spatially correlated channels," *IEEE Trans. Wireless Commun.*, vol. 20, no. 10, pp. 6451–6466, Oct. 2021.

[45] A. Duel-Hallen, "Fading channel prediction for mobile radio adaptive transmission systems," *Proc. IEEE*, vol. 95, no. 12, pp. 2299–2313, Dec. 2007.

[46] K. Ntontin et al., "Wireless energy harvesting for autonomous reconfigurable intelligent surfaces," *IEEE Trans. Green Commun. Netw.*, vol. 7, no. 1, pp. 114–129, Mar. 2023.
[47] Y. Mao, B. Clerckx, and V. O. K. Li, "Rate-splitting multiple access for downlink communication systems: Bridging, generalizing, and outperforming SDMA and NOMA," *EURASIP J. Wireless Commun. Netw.*, vol. 2018, no. 1, pp. 1–54, Dec. 2018.
[48] E. Che, H. D. Tuan, and H. H. Nguyen, "Joint optimization of cooperative beamforming and relay assignment in multi-user wireless relay networks," *IEEE Trans. Wireless Commun.*, vol. 13, no. 10, pp. 5481–5495, Oct. 2014.
[49] V.-D. Nguyen, T. Q. Duong, H. D. Tuan, O.-S. Shin, and H. V. Poor, "Spectral and energy efficiencies in full-duplex wireless information and power transfer," *IEEE Trans. Commun.*, vol. 65, no. 5, pp. 2220–2233, May 2017.
[50] A. Ben-Tal and A. Nemirovski, *Lectures on Modern Convex Optimization*. Philadelphia, PA, USA: SIAM, 2001.
[51] S. W. Ellingson, "Path loss in reconfigurable intelligent surface-enabled channels," in *Proc. IEEE 32nd Annu. Int. Symp. Pers., Indoor Mobile Radio Commun. (PIMRC)*, Sep. 2021, pp. 829–835.
[52] M. Najafi, V. Jamali, R. Schober, and H. V. Poor, "Physics-based modeling and scalable optimization of large intelligent reflecting surfaces," *IEEE Trans. Commun.*, vol. 69, no. 4, pp. 2673–2691, Apr. 2021.
[53] B. R. Marks and G. P. Wright, "Technical note—A general inner approximation algorithm for nonconvex mathematical programs," *Oper. Res.*, vol. 26, no. 4, pp. 681–683, Aug. 1978.
[54] L. J. Greenstein, S. S. Ghassemzadeh, V. Erceg, and D. G. Michelson, "Ricean k-factors in narrow-band fixed wireless channels: Theory, experiments, and statistical models," *IEEE Trans. Veh. Technol.*, vol. 58, no. 8, pp. 4000–4012, Oct. 2009.
[55] Y. Zhang, J. Zhang, M. Di Renzo, H. Xiao, and B. Ai, "Reconfigurable intelligent surfaces with outdated channel state information: Centralized vs. distributed deployments," *IEEE Trans. Commun.*, vol. 70, no. 4, pp. 2742–2756, Apr. 2022.
[56] H. Yang, Z. Xiong, J. Zhao, D. Niyato, L. Xiao, and Q. Wu, "Deep reinforcement learning-based intelligent reflecting surface for secure wireless communications," *IEEE Trans. Wireless Commun.*, vol. 20, no. 1, pp. 375–388, Jan. 2021.

Progress Zivuku (Graduate Student Member, IEEE) received the B.Sc. degree in telecommunications engineering from the University of Tlemcen, Algeria, in 2018, and the M.Sc. degree in information and communication engineering from the University of Trento, Italy, in 2020. She is currently pursuing the Ph.D. degree with the SIGCOM Group, Interdisciplinary Centre for Security, Reliability and Trust (SnT), University of Luxembourg. Her research interests include reconfigurable intelligent surfaces (RIS), joint communication and sensing, resource allocation, signal processing, optimization algorithms for future wireless networks, and cooperative communications.

Steven Kisseleff (Senior Member, IEEE) received the M.Sc. degree in information technology from the Technical University of Kaiserslautern, Germany, in 2011, and the Ph.D. degree in electrical engineering from the Friedrich-Alexander University of Erlangen-Nürnberg (FAU), Germany, in 2017. In 2018, he joined the SIGCOM Research Group, SnT, University of Luxembourg, where he is currently a Research Scientist. His research interests include design and optimization of satellite networks, multi-antenna systems, receiver synchronization, and the Internet of Things.

Van-Dinh Nguyen (Senior Member, IEEE) received the B.E. degree in electrical engineering from the Ho Chi Minh City University of Technology, Vietnam, in 2012, and the M.E. and Ph.D. degrees in electronic engineering from Soongsil University, Seoul, South Korea, in 2015 and 2018, respectively. Since September 2022, he has been an Assistant Professor with VinUniversity, Vietnam. He was a Research Associate with SnT, University of Luxembourg; a Post-Doctoral Researcher and a Lecturer with Soongsil University; a Post-Doctoral Visiting Scholar with the University of Technology Sydney; and a Ph.D. Visiting Scholar with Queen's University Belfast, U.K. He has authored or coauthored some 60 papers published in international journals and conference proceedings. His current research activity is focused on the mathematical modeling of 5G/6G cellular networks, edge/fog computing, and AI/ML solutions for wireless communications.

He received several best conference paper awards, the Exemplary Editor Award of IEEE COMMUNICATIONS LETTERS in 2019, the IEEE TRANSACTIONS ON COMMUNICATIONS Exemplary Reviewer in 2018, and the IEEE GLOBECOM Student Travel Grant Award in 2017. He has served as a reviewer for many top-tier international journals on wireless communications and a technical program committee member for several flag-ship international conferences in related fields. He is an Editor of the IEEE OPEN JOURNAL OF THE COMMUNICATIONS SOCIETY and IEEE SYSTEMS JOURNAL and a Senior Editor of IEEE COMMUNICATIONS LETTERS.

Wallace A. Martins (Senior Member, IEEE) received the degree in electronics engineer and the M.Sc. and D.Sc. degrees in electrical engineering from the Federal University of Rio de Janeiro (UFRJ), Rio de Janeiro, Brazil, in 2007, 2009, and 2011, respectively. He is a Full Professor with Institut Supérieur de l'Aéronautique et de l'Espace (ISAE-SUPAERO), Université de Toulouse, France. From 2019 to 2023, he was a Researcher with the Interdisciplinary Centre for Security, Reliability and Trust (SnT), University of Luxembourg. He was affiliated with UFRJ, as an Associate Professor, from 2013 to 2022. During this period, he also held roles as an Academic Coordinator of the electronics and computer engineering undergraduate course and the Deputy Department Chairman (DEL/Poli/UFRJ), from 2016 to 2017. He was also a Research Visitor with the University of Notre Dame, USA, in 2008; Université de Lille 1, France, in 2016; and Universidad de Alcalá, Spain, in 2018. His research interests include digital signal processing and telecommunications, with a focus on future wireless and satellite networks. He was a recipient of the Best Student Paper Award from EURASIP at EUSIPCO-2009, Glasgow, Scotland; the 2011 Best Brazilian D.Sc. Dissertation Award from Capes; and the Best Paper Award at SBrT-2020, Florianópolis, Brazil. He is a member (an Associate Editor) of the Editorial Boards of the IEEE SIGNAL PROCESSING LETTERS and the *EURASIP Journal on Advances in Signal Processing*.

Konstantinos Ntontin (Member, IEEE) received the Diploma degree in electrical and computer engineering from the University of Patras, Greece, in 2006, the M.Sc. degree in wireless systems from the Royal Institute of Technology (KTH), Sweden, in 2009, and the Ph.D. degree from the Technical University of Catalonia, Spain, in 2015. He is currently a Research Scientist with the SIGCOM Research Group, SnT, University of Luxembourg. In the past, he held research associate positions with the Electronic Engineering and Telecommunications Department, University of Barcelona; the Informatics and Telecommunications Department, University of Athens; and the National Centre of Scientific Research Demokritos. In addition, he held an internship position with Ericsson Eurolab Gmbh, Germany. His research interests are related to the physical layer of wireless telecommunications, with focus on performance analysis in fading channels, MIMO systems, array beamforming, transceiver design, and stochastic modeling of wireless channels.

Symeon Chatzinotas (Fellow, IEEE) received the M.Eng. degree in telecommunications from the Aristotle University of Thessaloniki, Greece, in 2003, and the M.Sc. and Ph.D. degrees in electronic engineering from the University of Surrey, U.K., in 2006 and 2009, respectively.

He is currently a Full Professor/the Chief Scientist I and the Head of the Research Group SIGCOM, Interdisciplinary Centre for Security, Reliability and Trust, University of Luxembourg. In parallel, he is an Adjunct Professor with the Department of Electronic Systems, Norwegian University of Science and Technology; and a Collaborating Scholar with the Institute of Informatics and Telecommunications, National Center for Scientific Research Demokritos. In the past, he has lectured as a Visiting Professor with the University of Parma, Italy; and contributed in numerous research and development projects for the Institute of Telematics and Informatics, Center of Research and Technology Hellas, and the Mobile Communications Research Group, Center of Communication Systems Research, University of Surrey. He has authored more than 800 technical papers in refereed international journals, conferences, and scientific books.

Dr. Chatzinotas received numerous awards and recognitions, including the IEEE Fellowship and an IEEE Distinguished Contributions Award. He is currently in the Editorial Board of IEEE TRANSACTIONS ON COMMUNICATIONS, IEEE OPEN JOURNAL OF VEHICULAR TECHNOLOGY, and the *International Journal of Satellite Communications and Networking*.

Björn Ottersten (Fellow, IEEE) received the M.S. degree in electrical engineering and applied physics from Linköping University, Linköping, Sweden, in 1986, and the Ph.D. degree in electrical engineering from Stanford University, Stanford, CA, USA, in 1990. He has held research positions with the Department of Electrical Engineering, Linköping University; the Information Systems Laboratory, Stanford University; Katholieke Universiteit Leuven, Leuven, Belgium; and the University of Luxembourg, Luxembourg. From 1996 to 1997, he was the Director of research with ArrayComm Inc., a start-up in San Jose, CA, USA, based on his patented technology. In 1991, he was appointed as a Professor of signal processing with the Royal Institute of Technology (KTH), Stockholm, Sweden, where he has been the Head of the Department for Signals, Sensors, and Systems, and the Dean of the School of Electrical Engineering. He is the Founding Director of the Interdisciplinary Centre for Security, Reliability and Trust, University of Luxembourg. He is a fellow of EURASIP and AAIA. He was a recipient of the IEEE Signal Processing Society Technical Achievement Award, the EURASIP Group Technical Achievement Award, and the European Research Council (ERC) Advanced Research Grant (twice). He has coauthored journal articles that received the IEEE Signal Processing Society Best Paper Award in 1993, 2001, 2006, 2013, and 2019; and nine IEEE conference papers best paper awards. He has been a Board Member of the IEEE Signal Processing Society and the Swedish Research Council. He serves on the boards for EURASIP, the Swedish Foundation for Strategic Research, and the ERC Scientific Council. He has served as the Editor-in-Chief for *EURASIP Signal Processing* and acted on the Editorial Boards for IEEE TRANSACTIONS ON SIGNAL PROCESSING, *IEEE Signal Processing Magazine*, IEEE OPEN JOURNAL FOR SIGNAL PROCESSING, *EURASIP Journal of Advances in Signal Processing*, and *Foundations and Trends in Signal Processing*.